$\bar{p}$ elastic scattering off light nuclei

Paolo Finelli
University of Bologna and INFN

Contacts:
paolo.finelli@unibo.it

in collaboration with M. Vorabbi (TRIUMF), C. Giusti (Pavia) and P. Navratil (TRIUMF)

Motivation

Past experiments

EXPERIMENTS AT THE LOW-ENERGY ANTIPROTON RING (LEAR)

Th. Walcher

"A pronounced diffractive pattern is visible that can be reproduced very well by an optical potential with a ***strong absorptive imaginary part*** *and a* ***rather shallow attractive real part****.*

Evidently, such a potential is well defined ***only at the surface*** *of the nucleus because of the strong absorption. The inner part of the nucleus plays practically no role since the antiprotons are essentially absorbed at ranges where the nuclear density is 10% of the central value."*

many-body effects suppressed?

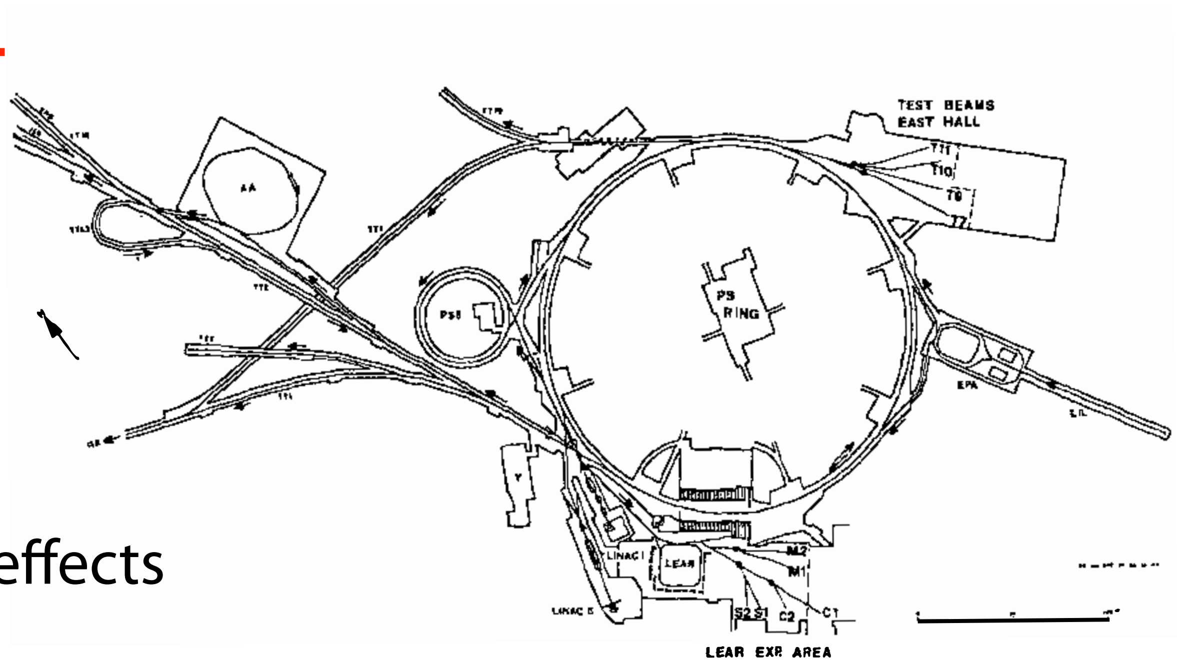

Figure 3 The PS, AA, and LEAR accelerator complex at CERN.

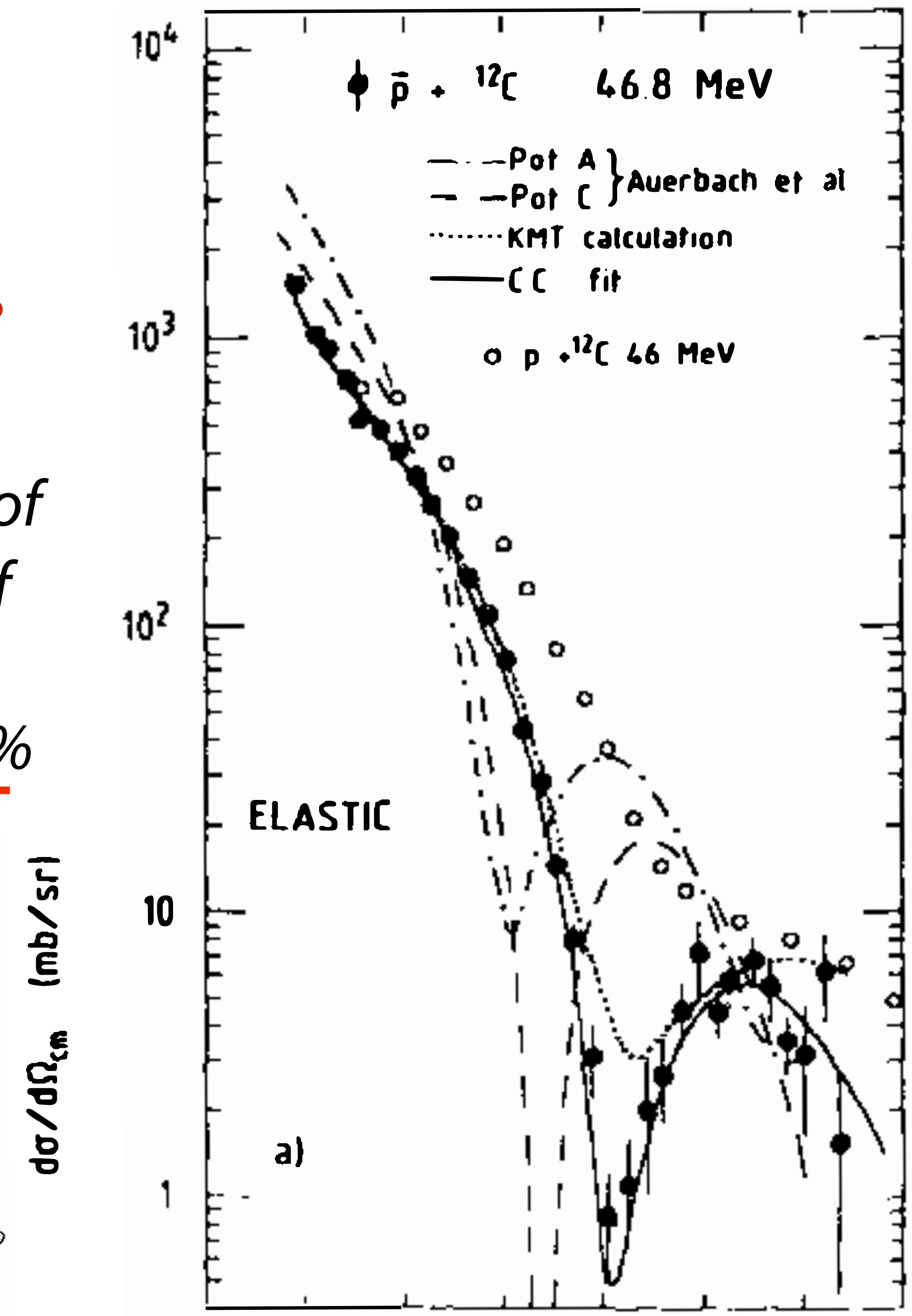

Ann. Rev. Nucl. Part. Sci. 1988. 38: 67–95

Phenomenological interpretations (~fits, no predictions)

Phenomenological model analysis of elastic and inelastic scattering of ≈ 180 MeV antiprotons from various nuclei

D. C. Choudhury and T. Guo
Department of Physics, Polytechnic University, Brooklyn, New York 11201

PRC 39 (1987) 1883

MICROSCOPIC ANALYSIS OF ANTIPROTON-NUCLEUS ELASTIC SCATTERING

S. ADACHI[1] and H.V. VON GERAMB

NPA 470 (1987) 461

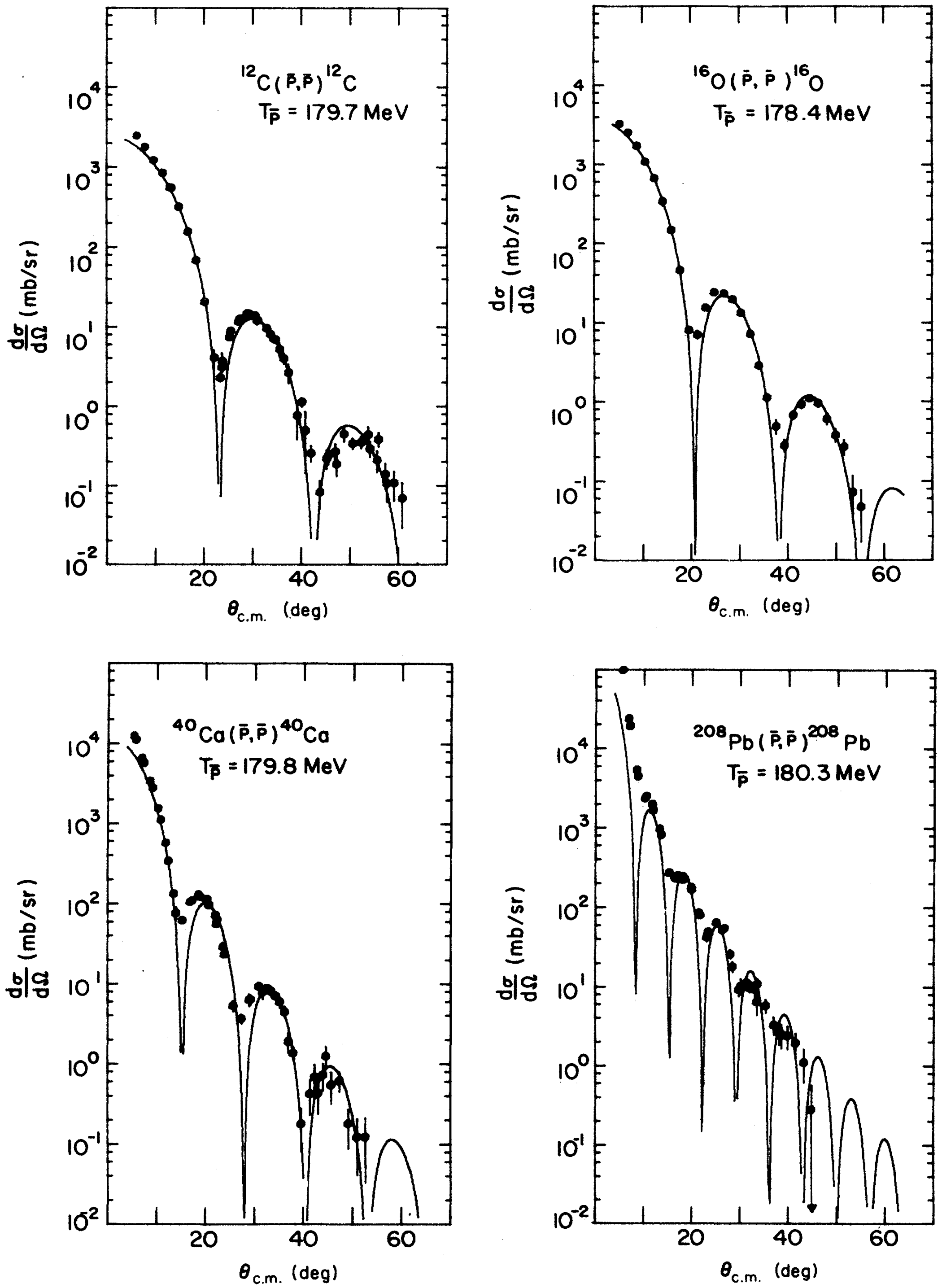

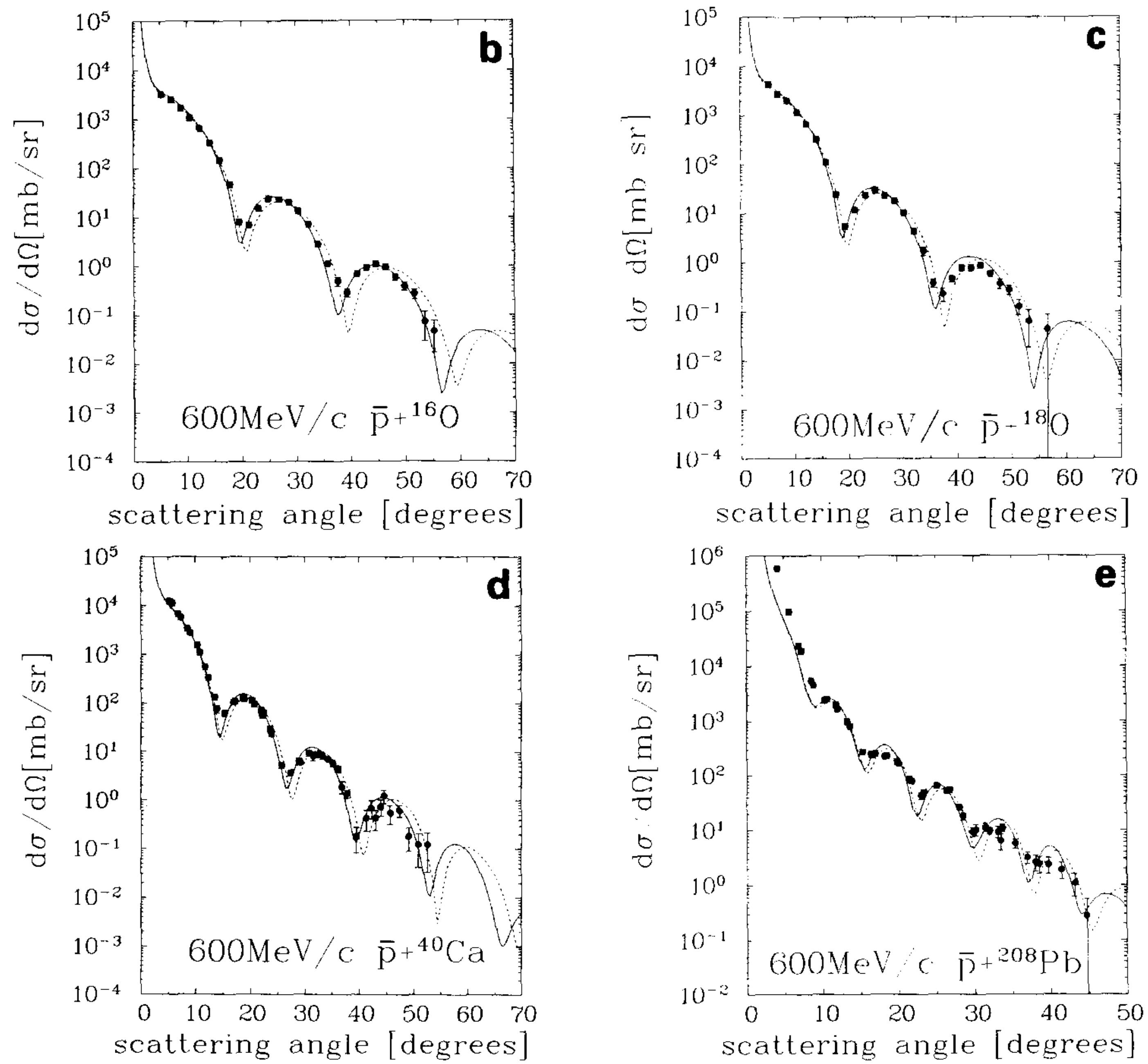

Phenomenological interpretations (~fits, no predictions)

Antiproton-nucleus elastic and inelastic scattering at intermediate energies

Zhang Yu-shun,[1,2] Liu Ji-feng,[3] B. A. Robson,[3] and Li Yang-guo[2]
[1]*CCAST (World Laboratory) Center of Theoretical Physics, P.O. Box 8730, 100 080 Beijing, China*
[2]*Institute of High Energy Physics, Academia Sinica, P.O. Box 918(4-1), 100 039 Beijing, China*
nt of Theoretical Physics, Research School of Physical Sciences and Engineering, The Australian National
Canberra, Australian Capital Territory 0200, Australia

PRC 54 (1996) 332

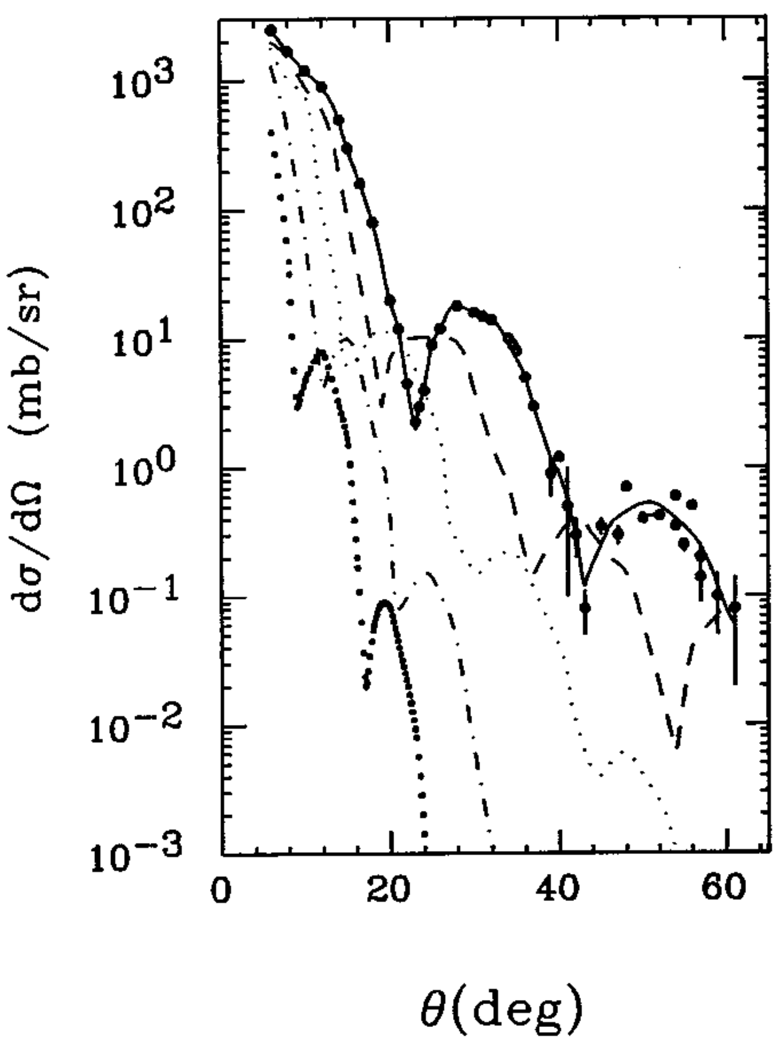

FIG. 2. Differential cross section for $\bar{p}$ elastic scattering on ^{12}C. —— 179.7 MeV, - - - - 294.8 MeV, ….. 508 MeV, –.–.–. 1070 MeV, and … … … 1833 MeV.

…and many others

Elastic scattering, polarization and absorption of relativistic antiprotons on nuclei

A.B. Larionov [a,b,*], H. Lenske [a]

NPA 957 (2017) 450

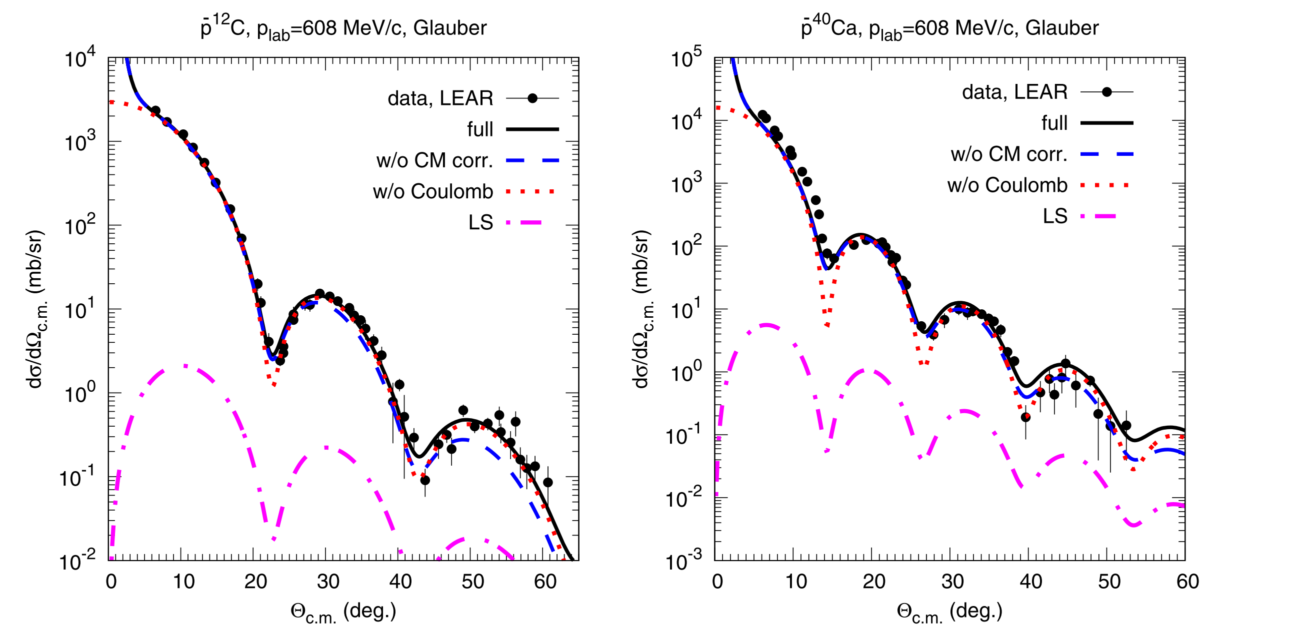

Fig. 2. Angular differential cross section of $\bar{p}$ elastic scattering at 608 MeV/c on ^{12}C, ^{40}Ca, and ^{208}Pb. Full GM calculation is shown by solid line. The dashed and dotted lines show, respectively, the results without recoil correction ($H_{\rm cm}(q) = 1$, Eq. (54)) and without Coulomb correction ($\xi = 0$, Eq. (22)). The dot-dashed line shows the contribution of the spin–orbit amplitude G to the differential cross section, Eq. (44). Experimental data are from ref. [46].

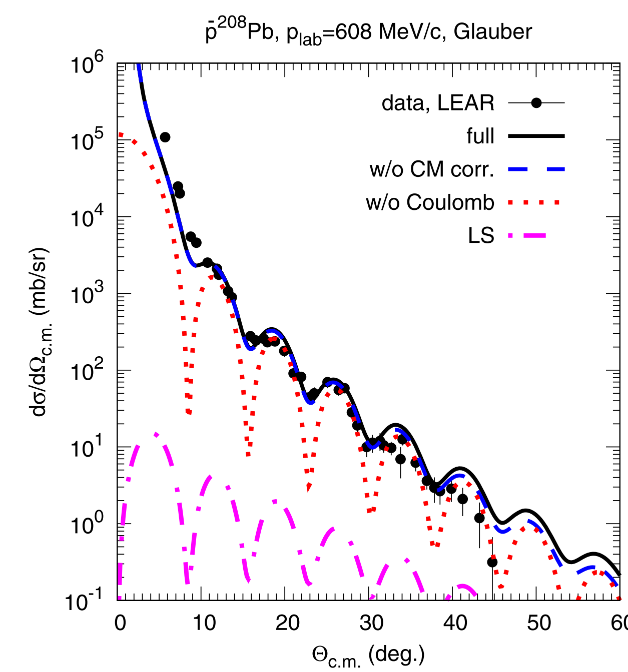

Phenomenological interpretations (~fits, no predictions)

Antiproton-nucleus elastic and inelastic scattering at intermediate energies

Zhang Yu-shun,[1,2] Liu Ji-feng,[3] B. A. Robson,[3] and Li Yang-guo[2]
[1]CCAST (World Laboratory) Center of Theoretical Physics, P.O. Box 8730, 100 080 Beijing, China
[2]Institute of High Energy Physics, Academia Sinica, P.O. Box 918(4-1), 100 039 Beijing, China
nt of Theoretical Physics, Research School of Physical Sciences and Engineering, The Australian National
Canberra, Australian Capital Territory 0200, Australia

PRC 54 (1996) 332

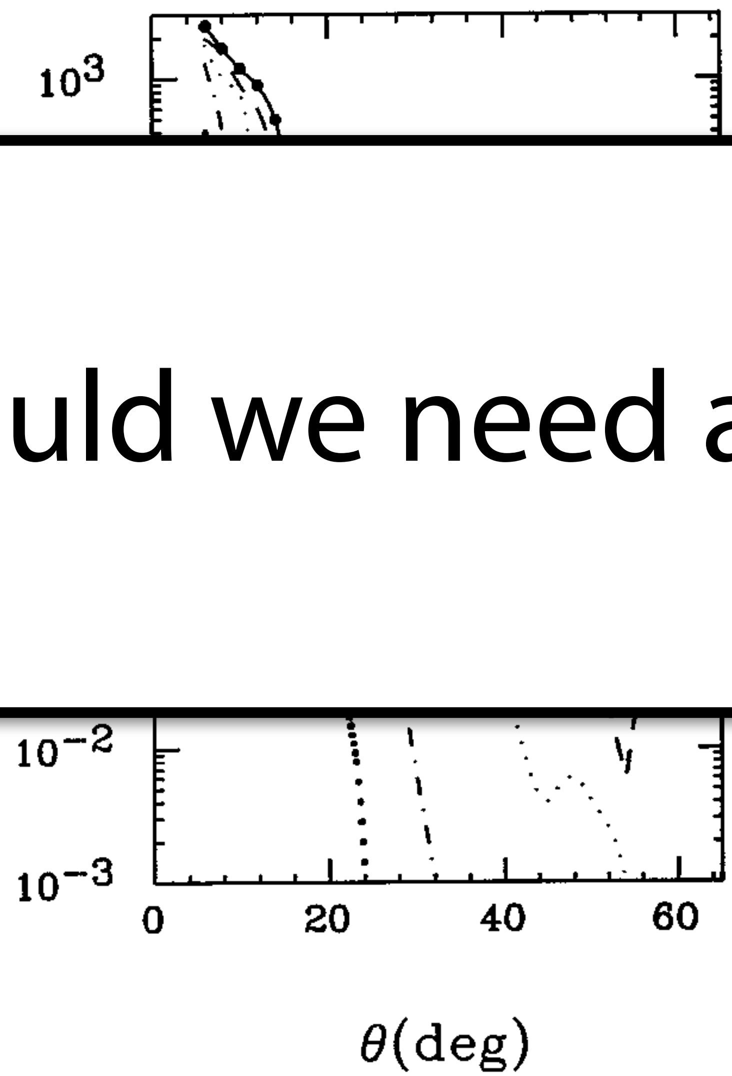

FIG. 2. Differential cross section for $\bar{p}$ elastic scattering on ^{12}C. —— 179.7 MeV, - - - - 294.8 MeV, ….. 508 MeV, –.–.–. 1070 MeV, and … … … 1833 MeV.

Elastic scattering, polarization and absorption of relativistic antiprotons on nuclei

A.B. Larionov [a,b,*], H. Lenske [a]

NPA 957 (2017) 450

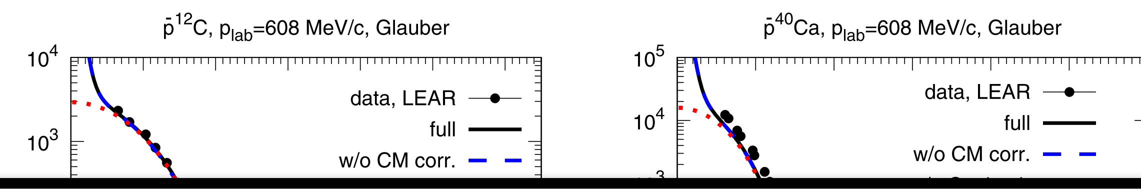

Should we need a full microscopic approach?

of the spin–orbit amplitude G to the differential cross section, Eq. (44). Experimental data are from ref. [46].

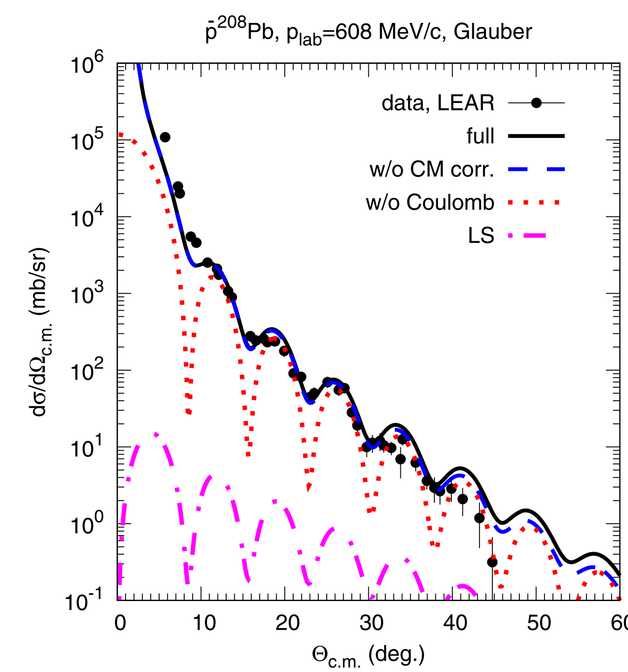

Chiral potentials

1. QCD symmetries are consistently respected
2. Systematic expansion (order by order you know exactly the terms to be included)
3. Theoretical errors
4. Two- and three-body forces belong to the same framework

Phenomenological potentials

1. QCD symmetries are not respected
2. Expansion determined by phenomenology (add whatever you need). A lot of freedom
3. Errors can't be estimated
4. Two- and three-body forces are not related one to each other

At the same time, from a theoretical point of view, it is important **to constrain** and **to test** the most recent chiral potentials

Convergence

Predictive power

Accuracy

Method

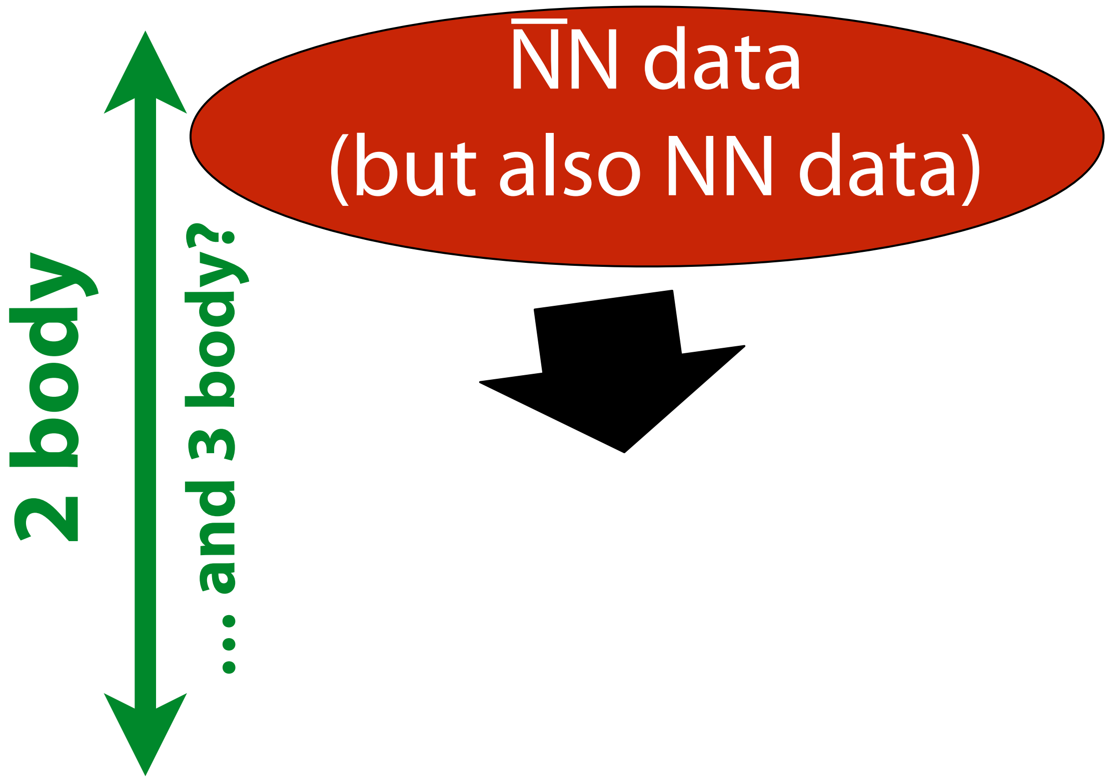

Nuclear reaction theory relies on reducing the many-body problem to a problem with few degrees of freedom: **optical potentials**.

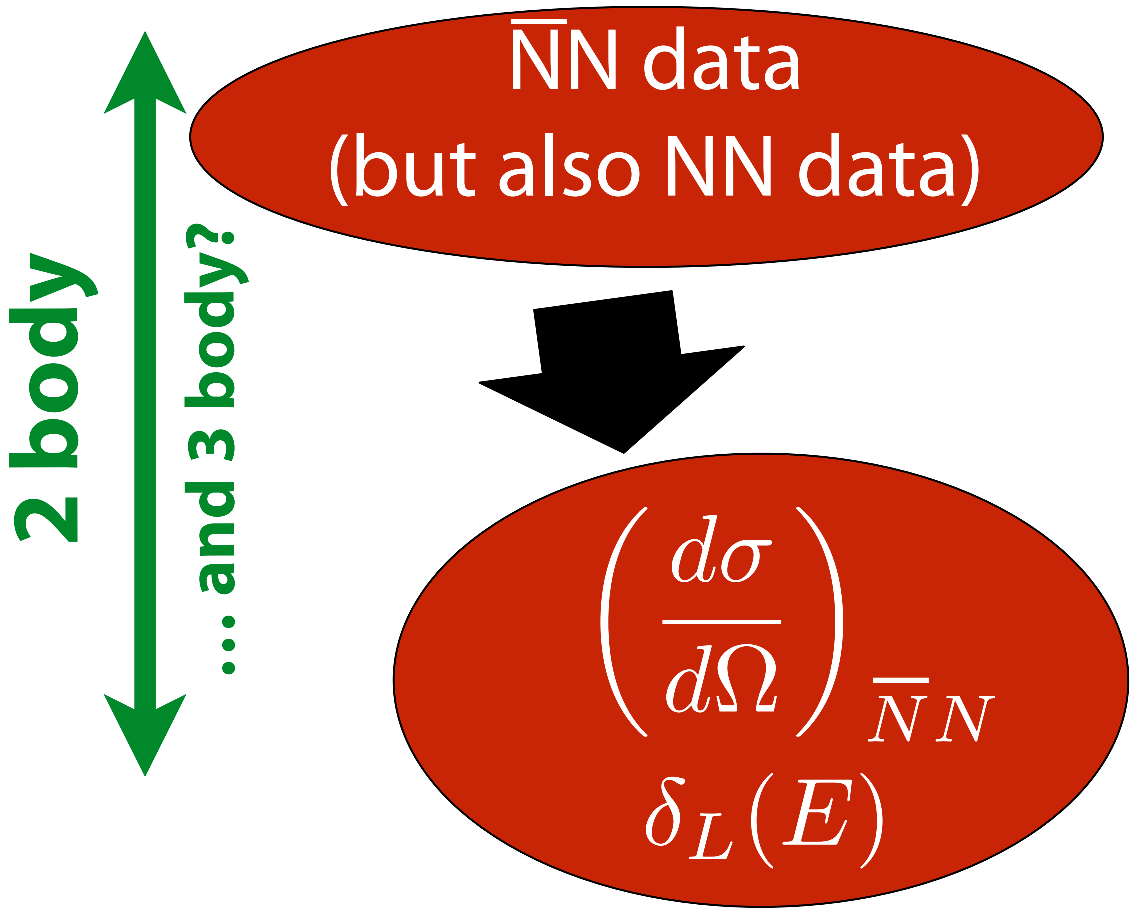

Nuclear reaction theory relies on reducing the many-body problem to a problem with few degrees of freedom: **optical potentials**.

$\overline{\text{N}}$N data
(but also NN data)

$$\left(\frac{d\sigma}{d\Omega}\right)_{\overline{N}N}$$

$$\delta_L(E)$$

$$V_{NN} = \begin{cases} G_{\overline{N}N} \\ t_{\overline{N}N} \end{cases}$$

2 body

... and 3 body?

Effective interaction

No fitting to empirical data

Nuclear reaction theory relies on reducing the many-body problem to a problem with few degrees of freedom: **optical potentials**.

Nuclear reaction theory relies on reducing the many-body problem to a problem with few degrees of freedom: **optical potentials**.

2 body

… and 3 body?

$\bar{N}N$ data
(but also NN data)

$$\left(\frac{d\sigma}{d\Omega}\right)_{\bar{N}N}$$
$$\delta_L(E)$$

Effective interaction

$$V_{NN} = \begin{cases} G_{\bar{N}N} \\ t_{\bar{N}N} \end{cases}$$

No fitting to empirical data

$\bar{N}+A$

More predictive power where no exp. data are available

$$U_{opt}(\boldsymbol{k}', \boldsymbol{k}, E)$$

$$\left(\frac{d\sigma}{d\Omega}\right)_{\bar{N}A}$$
$$A_y$$

Model

The general goal when solving the scattering problem of a antinucleon (or a nucleon) from a nucleus is to solve the corresponding **Lippmann-Schwinger equation** for the many-body transition amplitude T

$$T = V + V G_0(E) T$$

all two-body interactions

$$V = \sum_{i=1}^{A} v_{0i}$$

Green Function propagator

$$G_0(E) = \frac{1}{E - H_0 + i\epsilon}$$

where

$$H_0 = h_0 + H_A$$

$$H_A \left|\Phi_A\right\rangle = E_A \left|\Phi_A\right\rangle$$ **target Hamiltonian**

$$h_0$$ **kinetic term of the projectile**

for the nucleon-nucleus case see
Vorabbi, Giusti and Finelli, Phys. Rev. C 93, 034619 (2016)

The general goal when solving the scattering problem of a antinucleon (or a nucleon) from a nucleus is to solve the corresponding **Lippmann-Schwinger equation** for the many-body transition amplitude T

$$T = V + V G_0(E) T$$

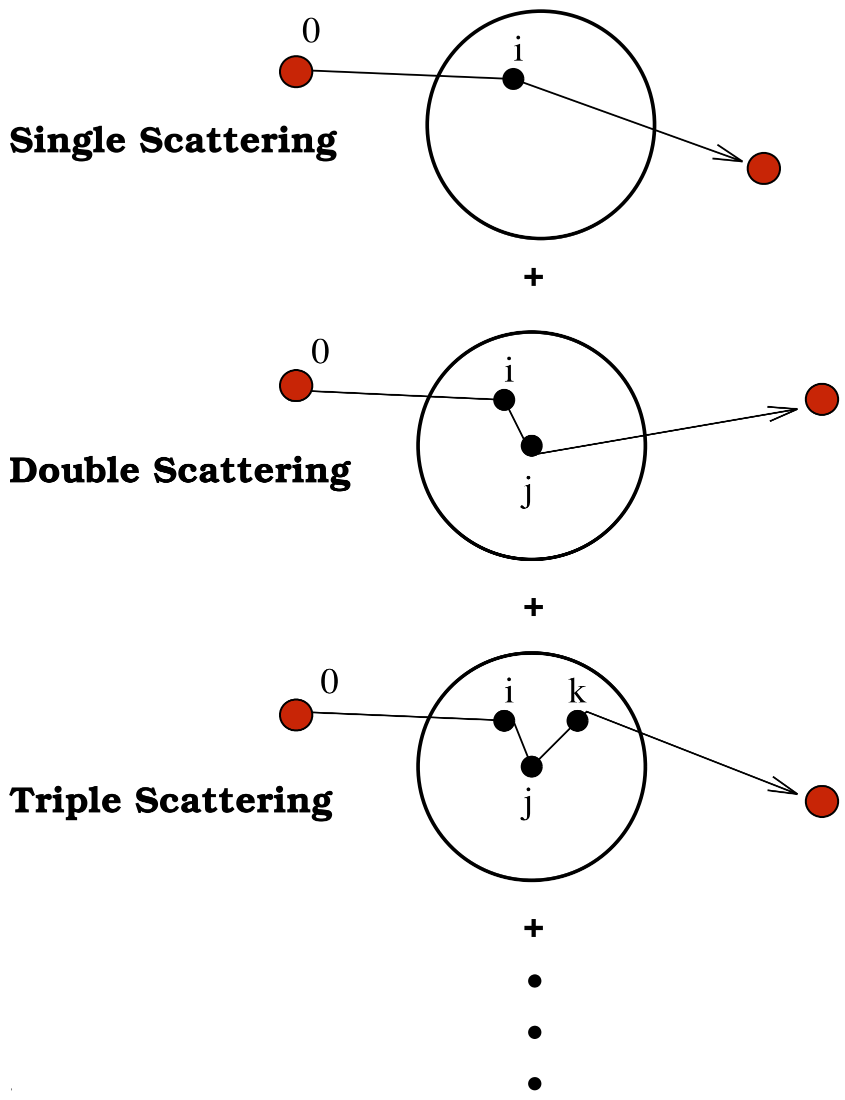

Vorabbi, Giusti and Finelli, Phys. Rev. C 93, 034619 (2016)

The general goal when solving the scattering problem of a antinucleon (or a nucleon) from a nucleus is to solve the corresponding **Lippmann-Schwinger equation** for the many-body transition amplitude T

$$T = V + VG_0(E)T$$

Spectator expansion
two particle interaction dominates the scattering process

$$T = \sum_{i=1} T_{0i}$$

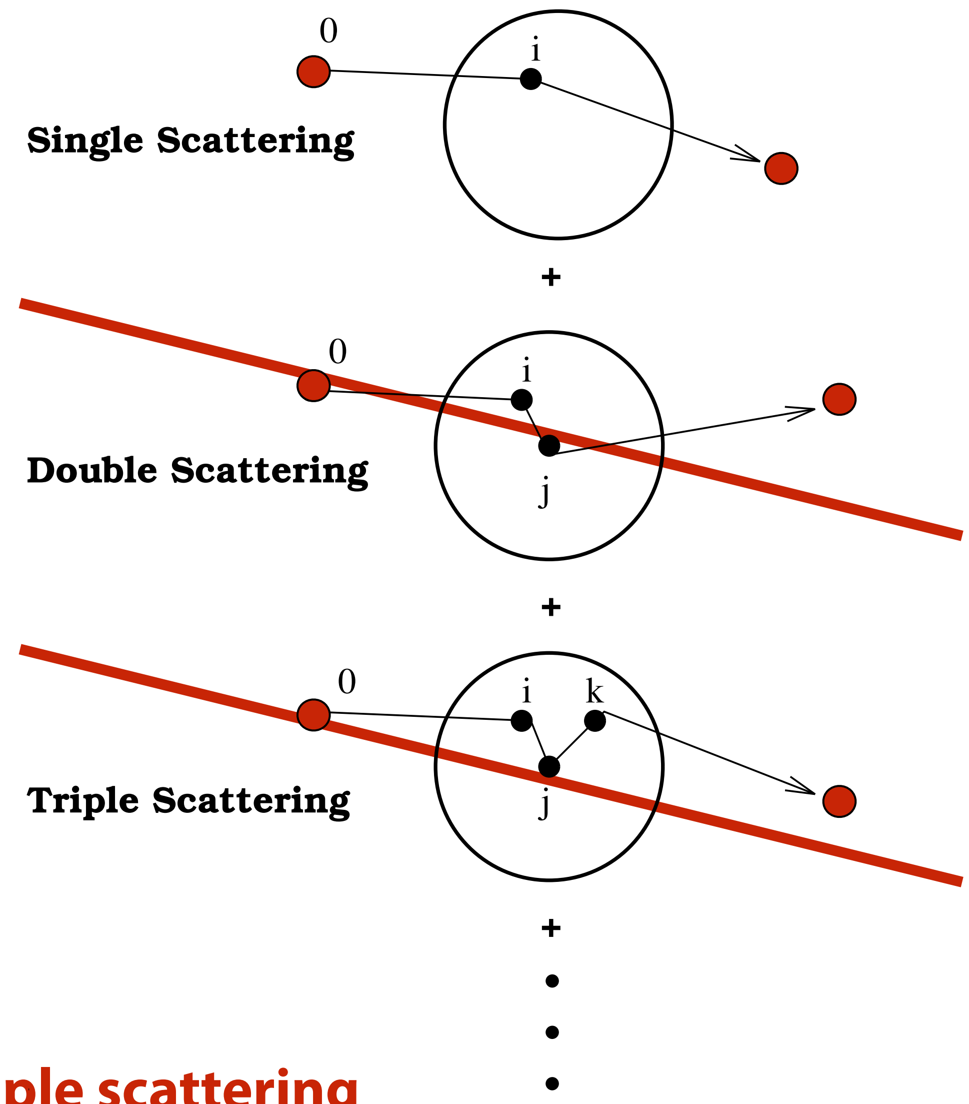

$$T_{0i} = v_{0i} + v_{0i}G_0(E)T,$$

$$\begin{aligned} T_{0i} &= v_{0i} + v_{0i}G_0(E)\sum_j T_{0j} \\ &= v_{0i} + v_{0i}G_0(E)T_{0i} + v_{0i}G_0(E)\sum_{j\neq i} T_{0j} \\ (1 - v_{0i}G_0(E))T_{0i} &= v_{0i} + v_{0i}G_0(E)\sum_{j\neq i} T_{0j} \end{aligned}$$

$$\boxed{T_{0i} = t_{0i} + t_{0i}G_0(E)\sum_{j\neq i} T_{0j}.}$$

Watson multiple scattering

The general goal when solving the scattering problem of a antinucleon (or a nucleon) from a nucleus is to solve the corresponding **Lippmann-Schwinger equation** for the many-body transition amplitude T

$$T = V + VG_0(E)T$$

Let's introduce the **optical potential U**

$$T = U + UG_0(E)PT$$

$$U = V + VG_0(E)QU$$

$$P + Q = 1$$

$$[G_0, P] = 0$$

In the case of elastic scattering,

P projects onto the elastic channel

$$P = \frac{|\Phi_A\rangle\langle\Phi_A|}{\langle\Phi_A|\Phi_A\rangle}$$

The general goal when solving the scattering problem of a antinucleon (or a nucleon) from a nucleus is to solve the corresponding **Lippmann-Schwinger equation** for the many-body transition amplitude T

$$T = V + VG_0(E)T$$

transition amplitude T for elastic scattering

$$T_{\mathrm{el}} = PUP + PUPG_0(E)T_{\mathrm{el}}$$

we need to calculate *PUP*

expressions for U are derived such that PUP can be calculated accurately without having to solve the complete many-body problem

The general goal when solving the scattering problem of a antinucleon (or a nucleon) from a nucleus is to solve the corresponding **Lippmann-Schwinger equation** for the many-body transition amplitude T

$$T_{\mathrm{el}} = PUP + PUPG_0(E)T_{\mathrm{el}}$$

$$U = \sum_{i=1}^{A} \tau_i + \sum_{i,j\neq i}^{A} \tau_{ij} + \sum_{i,j\neq i,k\neq i,j}^{A} \tau_{ijk} + \cdots$$

$$\begin{aligned} \hat{\tau}_i &= v_{0i} + v_{0i} G_0(E) \hat{\tau}_i \\ &= \tau_{0i} + \tau_{0i} G_0(E) P \hat{\tau}_{0i}. \end{aligned}$$

$$\begin{aligned} \langle \Phi_A | \tau_i | \Phi_A \rangle &= \langle \Phi_A | \hat{\tau}_i | \Phi_A \rangle - \langle \Phi_A | \hat{\tau}_i | \Phi_A \rangle \\ &\times \frac{1}{(E - E_A) - h_0 + i\epsilon} \langle \Phi_A | \tau_i | \Phi_A \rangle \end{aligned}$$

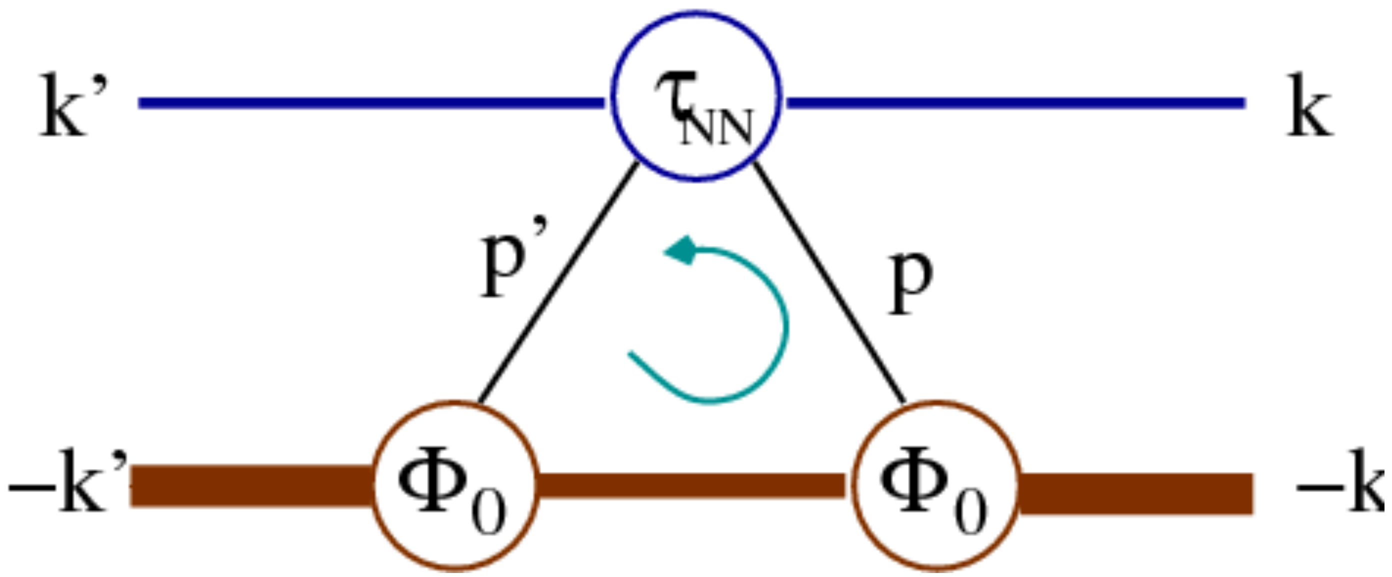

The general goal when solving the scattering problem of a antinucleon (or a nucleon) from a nucleus is to solve the corresponding **Lippmann-Schwinger equation** for the many-body transition amplitude T

$$T_{\mathrm{el}} = PUP + PUPG_0(E)T_{\mathrm{el}}$$

$$U = \sum_{i=1}^{A} \tau_i + \sum_{i,j\neq i}^{A} \tau_{ij} + \sum_{i,j\neq i,k\neq i,j}^{A}$$

$$\begin{aligned} \hat{\tau}_i &= v_{0i} + v_{0i}G_0(E)\hat{\tau}_i \\ &= \tau_{0i} + \tau_{0i}G_0(E)P\hat{\tau}_{0i}. \end{aligned}$$

$$\langle \Phi_A|\tau_i|\Phi_A\rangle = \langle \Phi_A|\hat{\tau}_i|\Phi_A\rangle - \langle \Phi_A|\hat{\tau}_i|\Phi_A\rangle \times \frac{1}{(E-E_A) - h_0 + i\epsilon} \langle \Phi_A|\tau_i|\Phi_A\rangle$$

Expanding the propagator $G_i(E) = \dfrac{1}{(E-E^i) - h_0 - h_i - W_i + i\epsilon}$

$$\hat{\tau}_i = v_{0i} + v_{0i}G_i(E)\hat{\tau}_i = t_{0i} + t_{0i}g_iW_iG_i(E)\hat{\tau}_i$$

free t matrix

$$t_{0i} = v_{0i} + v_{0i}g_it_{0i}$$

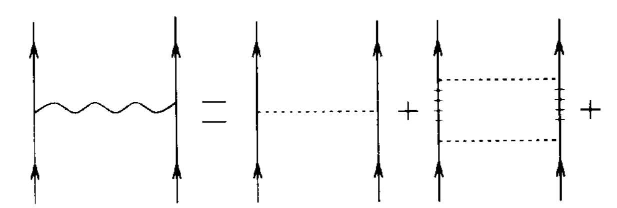

IMPULSE APPROXIMATION $\hat{\tau}_i \approx t_{0i}$

First-order optical potential

Kerman, McManus and Thaler, Ann. Phys. **8** (1959) 551 and many others

$$\boxed{\hat{U}(\boldsymbol{k}', \boldsymbol{k}; \omega) = (A-1)\,\langle \boldsymbol{k}', \Phi_A | t(\omega) | \boldsymbol{k}, \Phi_A \rangle}$$

$$\boldsymbol{q} \equiv \boldsymbol{k}' - \boldsymbol{k}\,, \qquad \boldsymbol{K} \equiv \frac{1}{2}(\boldsymbol{k}' + \boldsymbol{k})$$

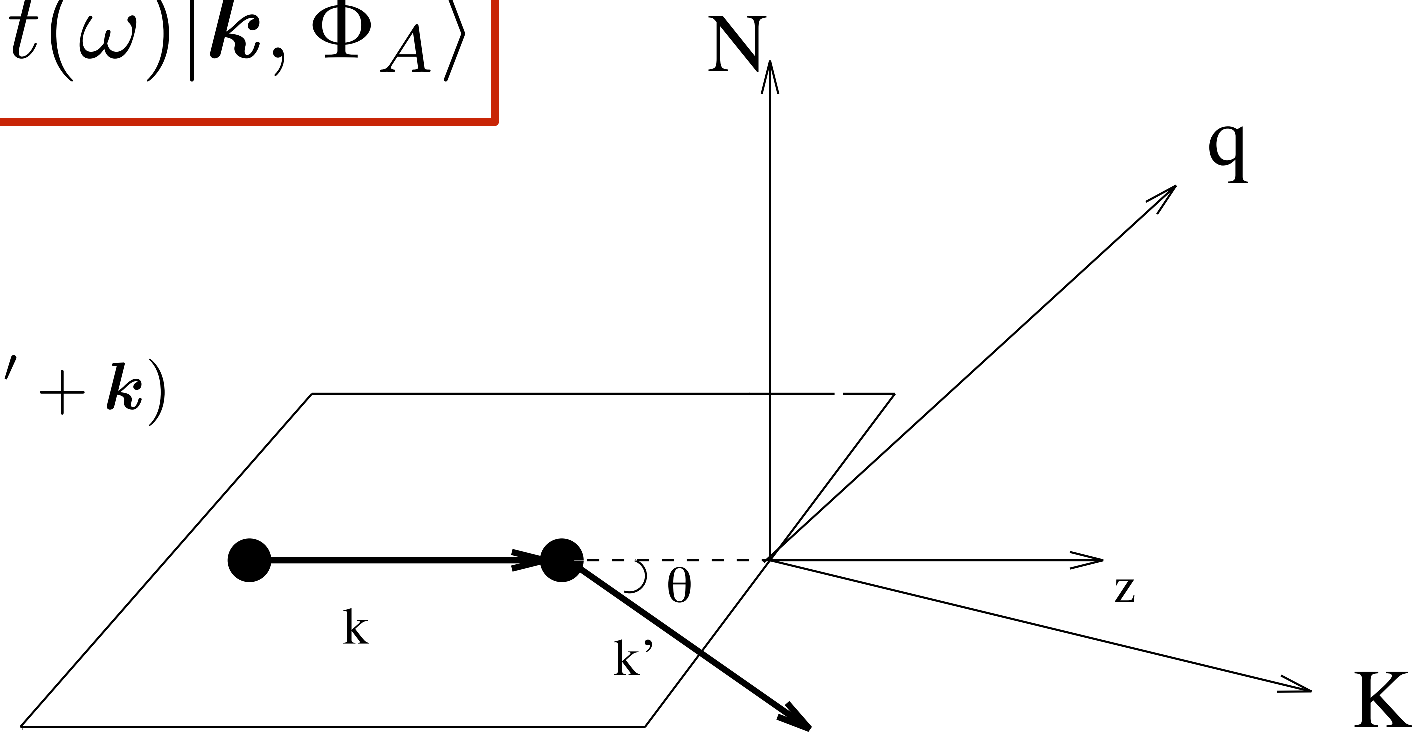

$$\hat{U}(\boldsymbol{q}, \boldsymbol{K}; \omega) = \frac{A-1}{A}\,\eta(\boldsymbol{q}, \boldsymbol{K}) \times \sum_{N=n,p} t_{\bar{p}N}\left[\boldsymbol{q}, \frac{A+1}{A}\boldsymbol{K}; \omega\right] \rho_N(q)$$

Optimum factorization factor

Møller factor

$$\eta(\boldsymbol{q}, \boldsymbol{K}) = \left[\frac{E_{\rm proj}(\boldsymbol{\kappa}')\,E_{\rm proj}(-\boldsymbol{\kappa}')\,E_{\rm proj}(\boldsymbol{\kappa})\,E_{\rm proj}(-\boldsymbol{\kappa})}{E_{\rm proj}(\boldsymbol{k}')\,E_{\rm proj}\left(-\frac{\boldsymbol{q}}{2} - \frac{\boldsymbol{K}}{A}\right)\,E_{\rm proj}(\boldsymbol{k})\,E_{\rm proj}\left(\frac{\boldsymbol{q}}{2} - \frac{\boldsymbol{K}}{A}\right)}\right]^{\frac{1}{2}}$$

First-order optical potential

$$\hat{U}(\boldsymbol{q},\boldsymbol{K};\omega) = \hat{U}^c(\boldsymbol{q},\boldsymbol{K};\omega) + \frac{i}{2}\boldsymbol{\sigma}\cdot\boldsymbol{q}\times\boldsymbol{K}\,\hat{U}^{ls}(\boldsymbol{q},\boldsymbol{K};\omega)$$

Central component

$$\hat{U}^c(\boldsymbol{q},\boldsymbol{K};\omega) = \frac{A-1}{A}\,\eta(\boldsymbol{q},\boldsymbol{K}) \times \sum_{N=n,p} t^c_{\bar{p}N}\left[\boldsymbol{q},\frac{A+1}{A}\boldsymbol{K};\omega\right]\rho_N(q)$$

Spin-orbit component

$$\hat{U}^{ls}(\boldsymbol{q},\boldsymbol{K};\omega) = \frac{A-1}{A}\,\eta(\boldsymbol{q},\boldsymbol{K})\left(\frac{A+1}{2A}\right) \times \sum_{N=n,p} t^{ls}_{\bar{p}N}\left[\boldsymbol{q},\frac{A+1}{A}\boldsymbol{K};\omega\right]\rho_N(q)$$

Full folding potential

Central component

$$U_c^{\alpha}(\boldsymbol{q}, \boldsymbol{K}; E) = \sum_{N=p,n} \int d\boldsymbol{P}\, \eta(\boldsymbol{q}, \boldsymbol{K}, \boldsymbol{P})\, t_{\alpha N}^{c} \left[\boldsymbol{q}, \frac{1}{2}\left(\frac{A+1}{A}\boldsymbol{K} + \sqrt{\frac{A-1}{A}}\boldsymbol{P}\right); E\right]$$
$$\times\, \bar{\rho}_N \left(\boldsymbol{P} + \frac{1}{2}\sqrt{\frac{A-1}{A}}\boldsymbol{q}, \boldsymbol{P} - \frac{1}{2}\sqrt{\frac{A-1}{A}}\boldsymbol{q}\right) ,$$

Spin-orbit component

$$U_{ls}^{\alpha}(\boldsymbol{q}, \boldsymbol{K}; E) = \sum_{N=p,n} \int d\boldsymbol{P}\, \eta(\boldsymbol{q}, \boldsymbol{K}, \boldsymbol{P})\, t_{\alpha N}^{ls} \left[\boldsymbol{q}, \frac{1}{2}\left(\frac{A+1}{A}\boldsymbol{K} + \sqrt{\frac{A-1}{A}}\boldsymbol{P}\right); E\right]$$
$$\times\, \bar{\rho}_N \left(\boldsymbol{P} + \frac{1}{2}\sqrt{\frac{A-1}{A}}\boldsymbol{q}, \boldsymbol{P} - \frac{1}{2}\sqrt{\frac{A-1}{A}}\boldsymbol{q}\right) .$$

Transition matrix

$$M(\boldsymbol{\kappa}', \boldsymbol{\kappa}, \omega) = \langle \boldsymbol{\kappa}' | M(\omega) | \boldsymbol{\kappa} \rangle = -4\pi^2 \mu \langle \boldsymbol{\kappa}' | t(\omega) | \boldsymbol{\kappa} \rangle$$

$$M = a + c(\boldsymbol{\sigma}_1 + \boldsymbol{\sigma}_2) \cdot \hat{\boldsymbol{n}} + m(\boldsymbol{\sigma}_1 \cdot \hat{\boldsymbol{n}})(\boldsymbol{\sigma}_2 \cdot \hat{\boldsymbol{n}}) + (g+h)(\boldsymbol{\sigma}_1 \cdot \hat{\boldsymbol{l}})(\boldsymbol{\sigma}_2 \cdot \hat{\boldsymbol{l}}) + (g-h)(\boldsymbol{\sigma}_1 \cdot \hat{\boldsymbol{m}})(\boldsymbol{\sigma}_2 \cdot \hat{\boldsymbol{m}})$$

$$\boxed{c_{\bar{p}N} = \frac{i}{f_{pN}\pi^2} \sum_{L=1}^{\infty} P_L^1(\cos\phi) \left[\left(\frac{2L+3}{L+1} \right) M_{LL}^{L+1,S=1} - \left(\frac{2L+1}{L(L+1)} \right) M_{LL}^{L,S=1} - \left(\frac{2L-1}{L} \right) M_{LL}^{L-1,S=1} \right]}$$

$$\boxed{a_{\bar{p}N} = \frac{1}{f_{pN}\pi^2} \sum_{L=0}^{\infty} P_L(\cos\phi) \Big[(2L+1)\, M_{LL}^{L,S=0} + (2L+1)\, M_{LL}^{L,S=1} + (2L+3)\, M_{LL}^{L+1,S=1} + (2L-1)\, M_{LL}^{L-1,S=1} \Big]}$$

The only relevant components for 0^+ nuclei, for $1/2^+$ more amplitudes must be included

Scattering observables

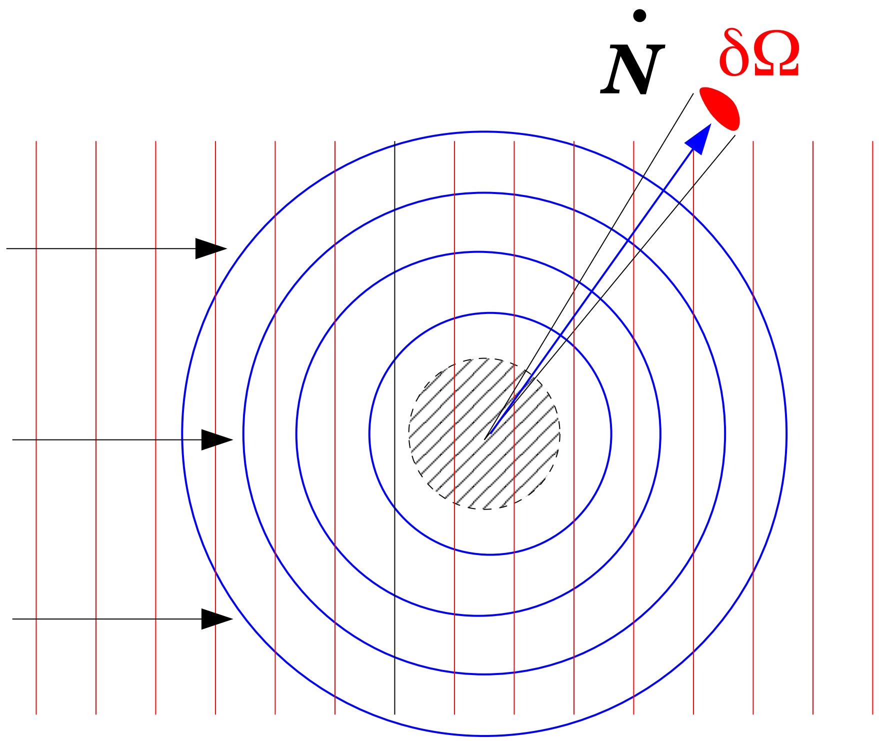

$$\dot{N} \sim \left\langle \frac{d\sigma}{d\Omega} \right\rangle \delta\Omega$$

$$\sigma(\theta) = \frac{d\sigma}{d\Omega} \sim \langle \mathbf{k}' | U | \psi_k \rangle$$

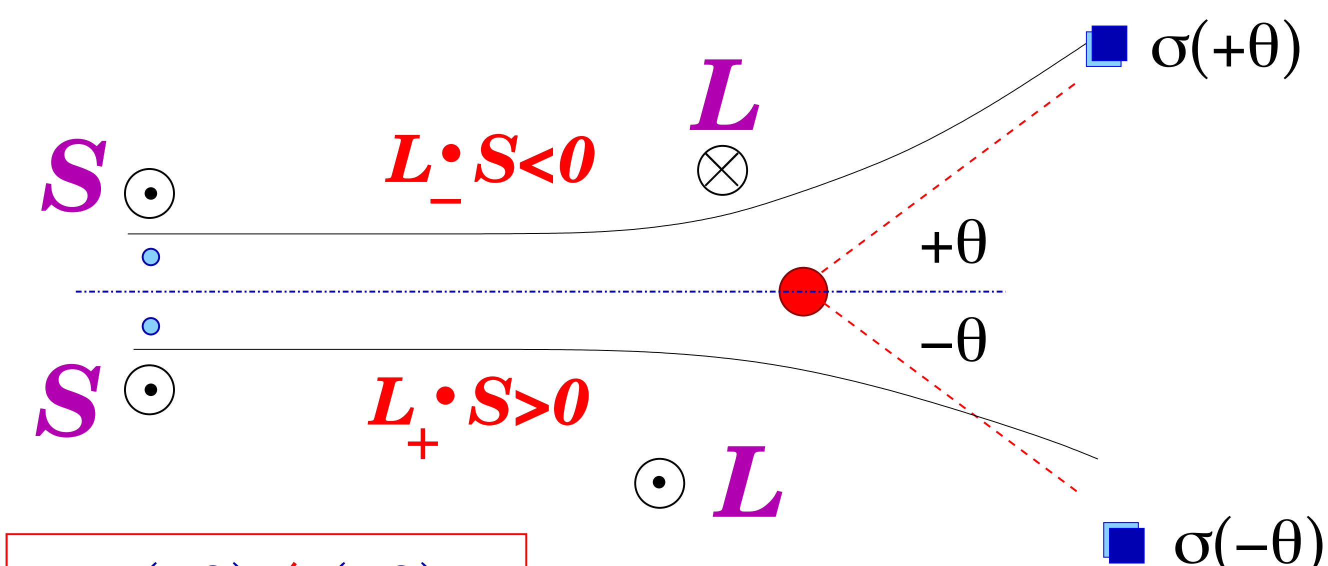

$\sigma(+\theta) \neq \sigma(-\theta)$

$U_c(r) + \mathbf{L}\cdot\mathbf{S}\, U_{so}(r)$

$$A_y(\theta) = \frac{\sigma(+\theta) - \sigma(-\theta)}{\sigma(+\theta) + \sigma(-\theta)}$$

It can be measured by sending a beam of polarised protons along ***+y*** and measure the total cross-section at angles ***θ*** and ***-θ*** in the scattering plane

Scattering observables

Spin-flip amplitude

$$M(k_0,\theta) = A(k_0,\theta) + \boldsymbol{\sigma}\cdot\underline{\hat{\mathbf{N}}\,C(k_0,\theta)}$$

$$A(\theta) = \frac{1}{2\pi^2}\sum_{L=0}^{\infty}\left[(L+1)F_L^{+}(k_0) + LF_L^{-}(k_0)\right]P_L(\cos\theta)$$

$$F_{LJ}(k_0) = -\frac{A}{A-1}4\pi^2\mu(k_0)\hat{T}_{LJ}(k_0,k_0;E)$$

$$C(\theta) = \frac{i}{2\pi^2}\sum_{L=1}^{\infty}\left[F_L^{+}(k_0) - F_L^{-}(k_0)\right]P_L(\cos\theta)$$

Differential cross section

$$\frac{d\sigma}{d\Omega}(\theta) = |A(\theta)|^2 + |C(\theta)|^2$$

Analyzing power

$$A_y(\theta) = \frac{2\mathrm{Re}[A^*(\theta)\,C(\theta)]}{|A(\theta)|^2 + |C(\theta)|^2}$$

Spin rotation

$$Q(\theta) = \frac{2\mathrm{Im}[A(\theta)\,C^*(\theta)]}{|A(\theta)|^2 + |C(\theta)|^2}$$

Rotation of the spin vector in the scattering plane, i.e. protons polarised along the ***+x*** axis have a finite probability of having the spin polarised along the **±** ***z*** axis after the collision

Inclusion of the Coulomb potential

Combine phase shifts from Coulomb and nuclear

$$\boxed{\sigma_L = \arg \Gamma\left[L + 1 + i\eta(k_0)\right]}$$

The central amplitude include a Coulomb component

$$A(k_0, \theta) = F^{c}_{\bar{p}t}(k_0, \theta) + \frac{1}{2\pi^2} \sum_{L=0}^{\infty} e^{2i\sigma_L} \left[(L+1)\bar{F}^{+}_{L}(k_0) + L\bar{F}^{-}_{L}(k_0)\right] P_L(\cos\theta)$$

$$F^{c}_{\bar{p}t}(k_0, \theta) = \frac{-\eta(k_0)\, \exp\left[2i\sigma_0 - i\eta(k_0)\ln(1-\cos\theta)\right]}{k_0(1-\cos\theta)}$$

Sommerfeld parameter

$$\eta(k) = \frac{\mu Z \alpha}{k}$$

$$u''_L(r) = \left[\frac{L(L+1)}{r^2} + \frac{2\mu}{\hbar^2}(V(r) - E)\right] u_L(r)$$

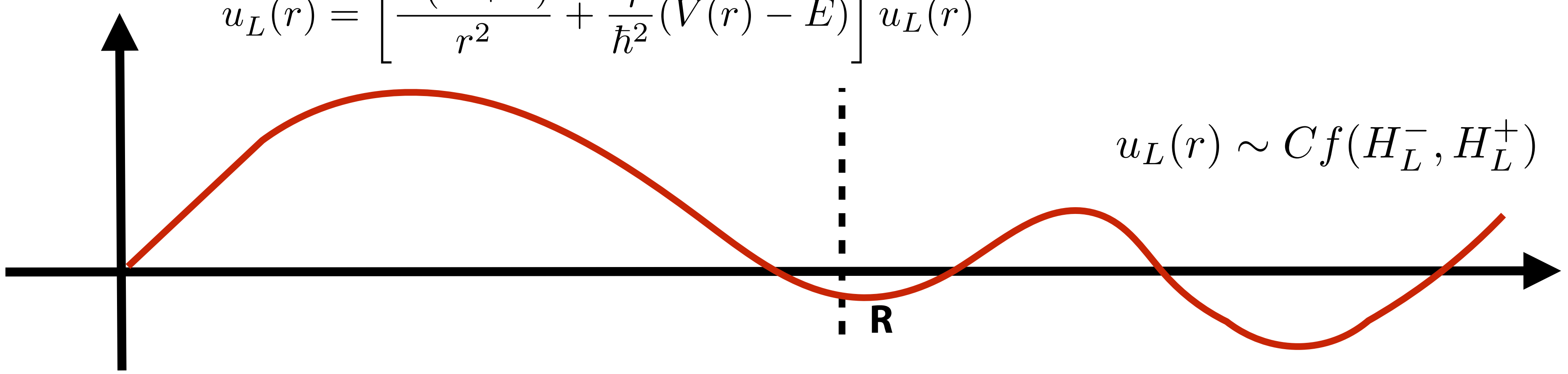

Do not add nuclear and Coulomb separately!

$$\bar{U}(\boldsymbol{k}', \boldsymbol{k}; \omega) = \langle \boldsymbol{k}' | \bar{U}(\omega) | \boldsymbol{k} \rangle = \langle \psi^{(+)}_c(\boldsymbol{k}') | \hat{U}(\omega) | \psi^{(+)}_c(\boldsymbol{k}) \rangle$$

Densities

Ab initio no core shell model

The basic idea of the NCSM is simply to treat **all A nucleons in a nucleus as active**: write down the Schrödinger equation for A nucleons and then solve it numerically.

Review
Ab initio no core shell model
Bruce R. Barrett[a], Petr Navrátil[b], James P. Vary[c,*]
Progress in Particle and Nuclear Physics 69 (2013) 131–181

This approach avoids essentially all of the difficulties of the perturbative approaches (like problems related to excitations of nucleons from the core).

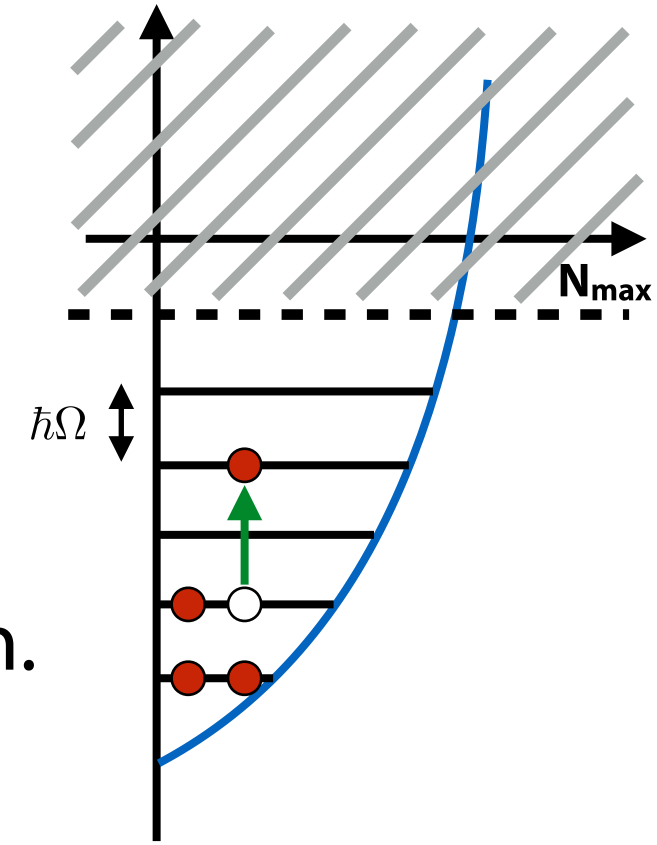

Being a non-perturbative approach, there are no difficulties related to convergence of such an expansion. It may also be formulated in terms of an **intrinsic Hamiltonian**, so as to **avoid spurious COM motion**.

Problems:
(1) need for **larger basis spaces**
(2) need for **effective many-body forces**, in order to treat all of the complexity of the excited-states.

Ab initio no core shell model

- In the ab initio no core shell model we consider a system of A point-like non-relativistic nucleons that interact by realistic two- or two- plus three-nucleon interactions.
- We employ NN potentials that fit nucleon–nucleon phase shifts with high precision up to a certain energy, typically up to 350 MeV.
- In the NCSM, **all the nucleons are considered active; there is no inert core like** in standard shell model calculations. Hence, the "no core" in the name of the approach.

$$H_A = T_{\mathrm{rel}} + \mathcal{V} = \frac{1}{A}\sum_{i<j}\frac{(\vec{p}_i - \vec{p}_j)^2}{2m} + \sum_{i<j}^{A} V_{\mathrm{NN},ij} + \sum_{i<j<k}^{A} V_{\mathrm{NNN},ijk},$$

m is the nucleon mass

$V_{NN,ij}$ is the NN interaction

$V_{NNN,ijk}$ is the three-nucleon interaction

Progress in Particle and Nuclear Physics 69 (2013) 131–181

Ab initio no core shell model: the basis

NCSM uses the harmonic-oscillator (HO) basis, truncated by a chosen **maximal total HO energy** (**N_{max}**) of the A-nucleon system. The reason behind the choice of the HO basis is the fact that this is the only basis that allows for the use of single-nucleon coordinates without violating the translational invariance of the system.

As a downside, one has to face the consequences of the incorrect asymptotic behavior of the HO basis.

$$\varphi_{nlm}(\vec{r};b) = R_{nl}(r;b)Y_{lm}(\hat{r}),$$

Jacobi's coordinate

$$|(nlsjt;\mathcal{N}\mathcal{L}\mathcal{J})JT\rangle.$$

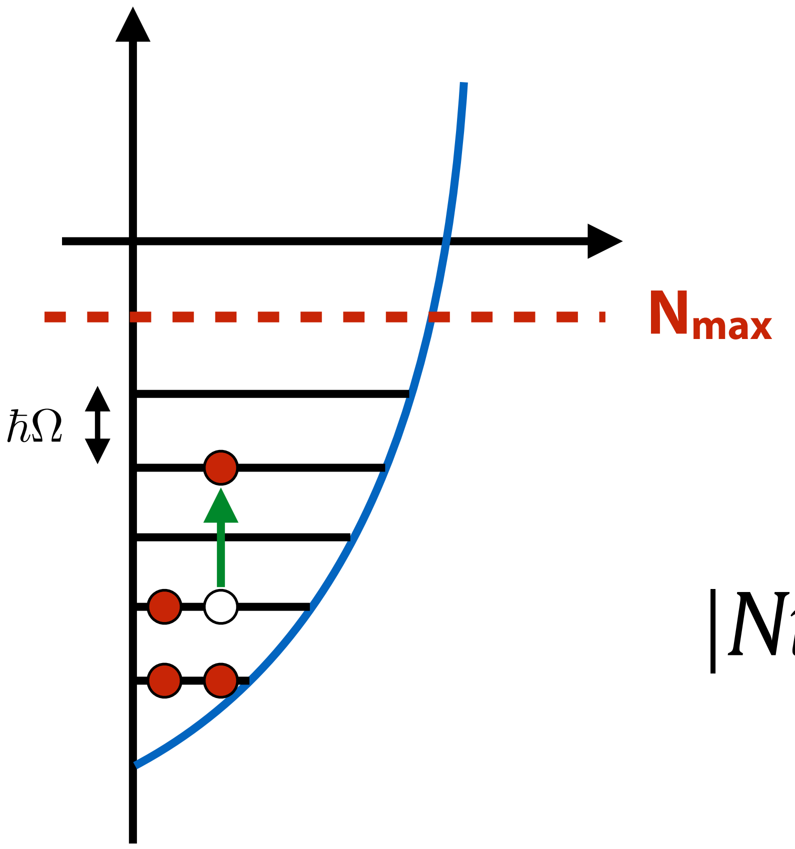

antisymmetrized states

$$|NiJT\rangle = \sum \langle nlsjt;\mathcal{N}\mathcal{L}\mathcal{J}||NiJT\rangle|(nlsjt;\mathcal{N}\mathcal{L}\mathcal{J})JT\rangle$$

Slater determinants for A greater than 3

Progress in Particle and Nuclear Physics 69 (2013) 131–181

Ab initio no core shell model: the interaction

Ab initio NCSM calculations uses a truncated HO basis but the nuclear interactions act in the full space. As long as one uses soft potentials, such as the V_{lowk} and SRG NN, convergent NCSM results can be obtained (<u>the similarity transformation softens the interactions and generates effective operators for all observables while preserving all experimental quantities in the low-energy domain</u>).

The situation is different when standard NN potentials that generate strong short-range correlations are used.

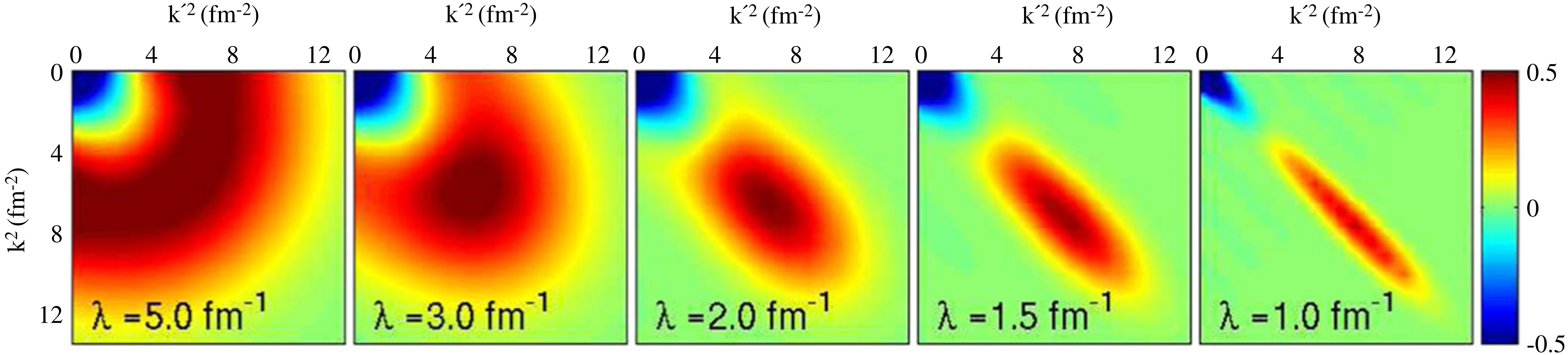

$$H_\lambda = U_\lambda H_{\lambda=\infty} U_\lambda^\dagger$$

$$\frac{dH_\lambda}{d\lambda} = -\frac{4}{\lambda^5}[[T_{\rm rel}, H_\lambda], H_\lambda]$$

The derived "effective" interactions still act among all A nucleons and preserve all the symmetries of the initial or "bare" NN +NNN interactions.

Progress in Particle and Nuclear Physics 69 (2013) 131–181

Ab initio no core shell model: the density matrix

$$\rho_{\mathrm{op}}(\vec{r},\vec{r}\,') = \sum_{i=1}^{A} (|\vec{r}\rangle\langle\vec{r}\,'|)^i = \sum_{i=1}^{A} \delta(\vec{r}-\vec{r}_i)\delta(\vec{r}\,'-\vec{r}\,'_i)$$

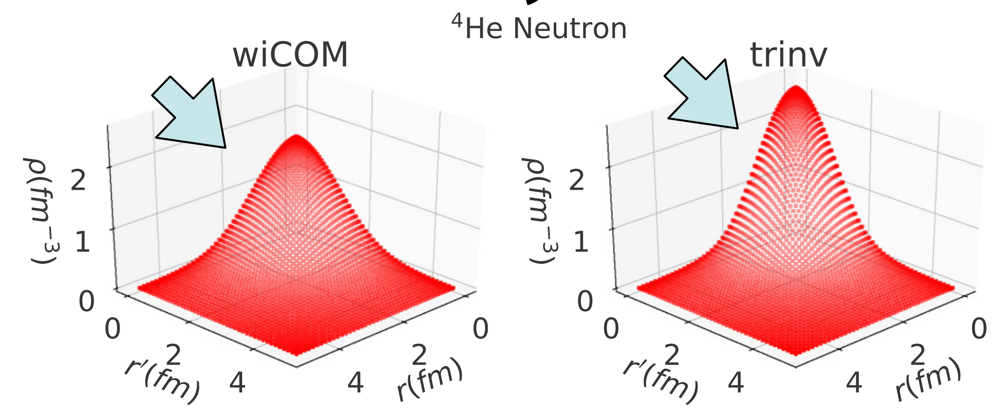

FIG. 1. Ground-state ^{4}He nonlocal neutron density calculated with an $N_{\max} = 14$ basis space, an oscillator frequency of $\hbar\Omega = 20$ MeV, and a flow parameter of $\lambda_{\mathrm{SRG}} = 2.0\ \mathrm{fm}^{-1}$.

wiCOM: COM contaminated density

trinv: translationally invariant density

The tremendous difference between the **trinv** density and the **wiCOM** density is easily recognizable at small r and r′. We notice that the trinv density has sharper features at peaks and tends to decay more rapidly than the wiCOM density. The COM contamination appears to suppress the nuclear density at small r and r ' values.

Notably, the COM term diminishes with A so we expect a reduction in the importance of its removal as we go to higher A-nucleon systems.

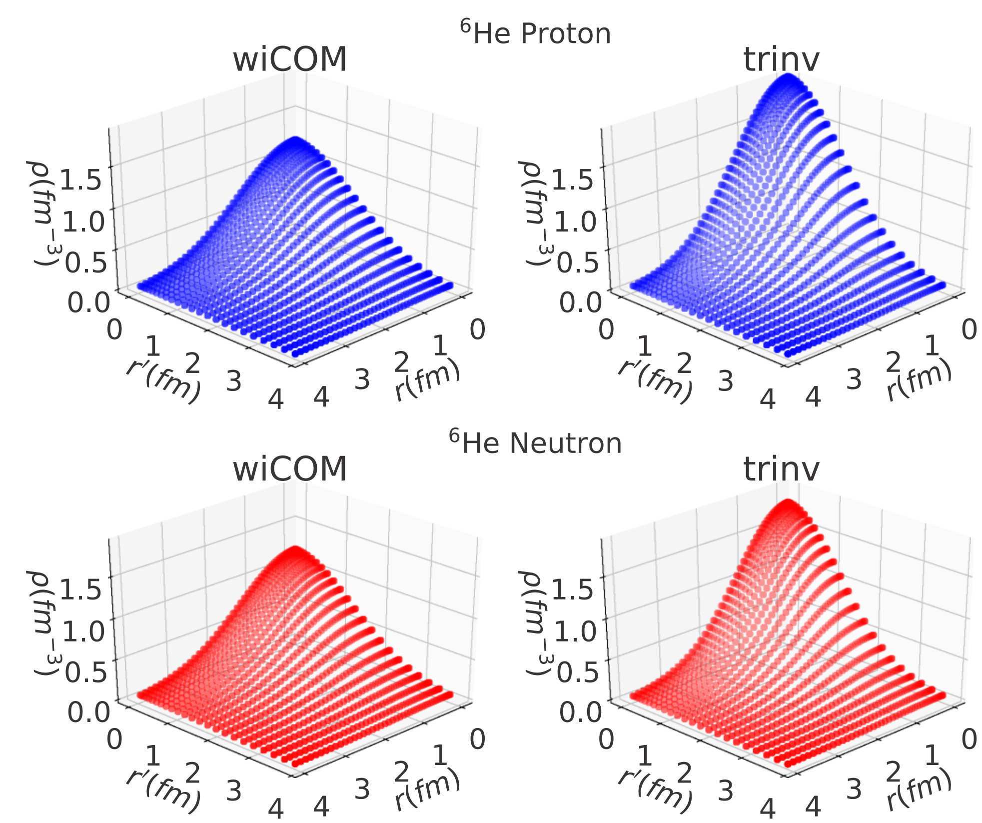

FIG. 2. Ground-state ^{6}He proton and neutron nonlocal densities calculated with a $N_{\max} = 12$ basis space, an oscillator frequency of $\hbar\Omega = 20$ MeV, and a flow parameter of $\lambda_{\mathrm{SRG}} = 2.0\ \mathrm{fm}^{-1}$. Proton densities are shown in blue and neutron densities are shown in red.

PHYSICAL REVIEW C **97**, 034619 (2018)

An alternative: matter densities from DFT

Typel and Wolter , Nuc. Phys. A **656** (1999) 331

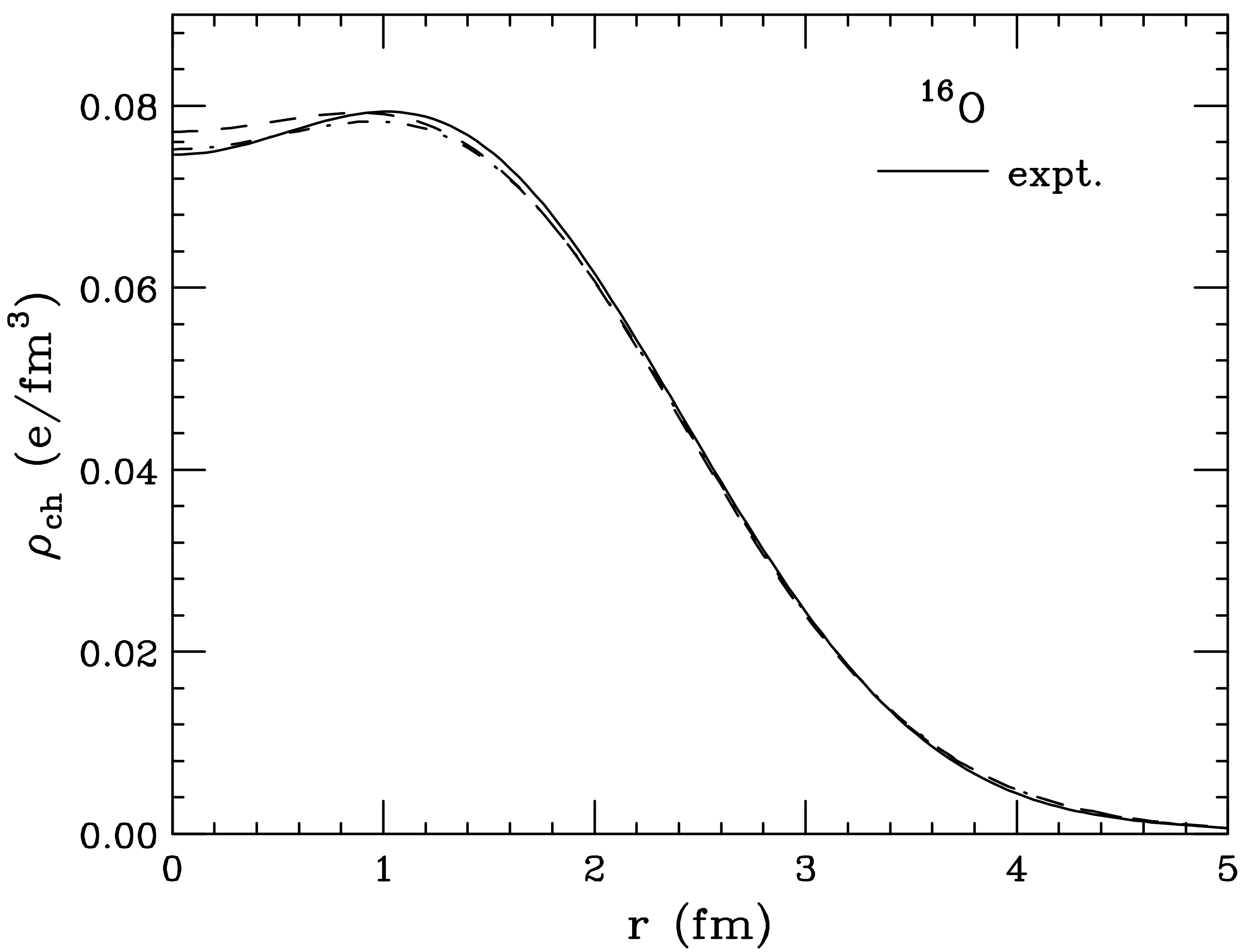

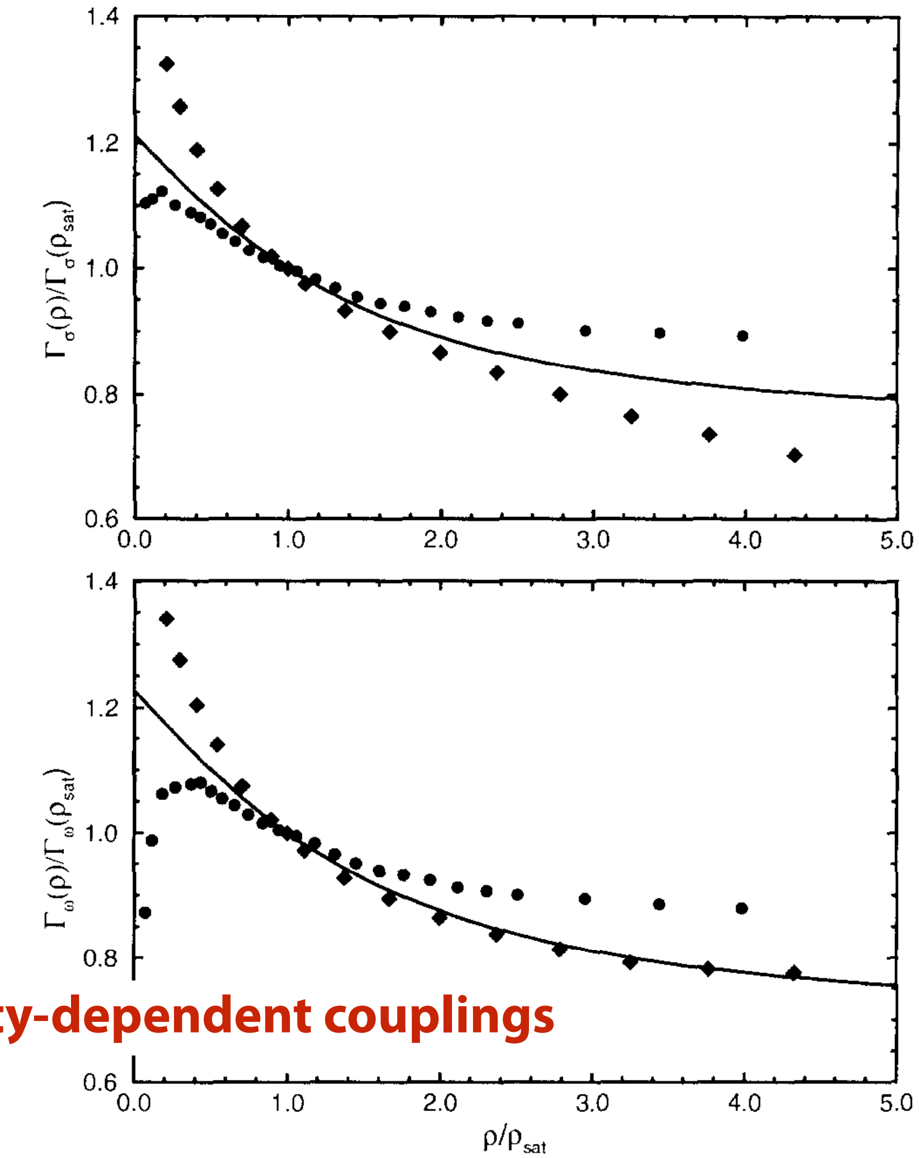

Density-dependent couplings

$$\mathcal{L} = \bar{\Psi}\left[\gamma^\mu\left(i\partial_\mu - \Gamma_\omega A_\mu^{(\omega)} - \Gamma_\varrho \frac{\boldsymbol{\tau}}{2}\cdot \boldsymbol{A}_\mu^{(\varrho)} - e\frac{1+\tau_3}{2}A_\mu^{(\gamma)}\right) - (m - \Gamma_\sigma \phi)\right]\Psi$$
$$+\frac{1}{2}\left[\partial_\mu\phi\partial^\mu\phi - m_\sigma^2\phi^2 - \frac{1}{2}F_{\mu\nu}^{(\omega)}F^{(\omega)\mu\nu} + m_\omega^2 A_\mu^{(\omega)}A^{(\omega)\mu}\right.$$
$$\left.-\frac{1}{2}\boldsymbol{F}_{\mu\nu}^{(\varrho)}\cdot\boldsymbol{F}^{(\varrho)\mu\nu} + m_\varrho^2\boldsymbol{A}_\mu^{(\varrho)}\cdot\boldsymbol{A}^{(\varrho)\mu} - \frac{1}{2}F_{\mu\nu}^{(\gamma)}F^{(\gamma)\mu\nu}\right]$$

DDME1 parametrization

T. Nikšić, D. Vretenar, P. Finelli and P. Ring
Phys. Rev. C **66** (2002) 024306

$\bar{N}N$ potentials

basic features of $\bar{\text{N}}$N potentials

In the limit where the neutron-to-proton mass difference can be neglected, as well as Coulomb corrections, the $\bar{\text{N}}$N system obeys isospin symmetry:

- antiproton–neutron is pure isospin I =1
- while p̄p and n̄n, with I_3 =0, are combinations of I =1 and I =0, namely

Antinucleon–nucleon interaction at low energy: scattering and protonium

Eberhard Klempt[a], Franco Bradamante[b], Anna Martin[b], Jean-Marc Richard[c,d,*]

Physics Reports 368 (2002) 119

$$|\bar{\mathrm{p}}\mathrm{p}\rangle = \frac{|I=1\rangle + |I=0\rangle}{\sqrt{2}}, \quad |\bar{\mathrm{n}}\mathrm{n}\rangle = \frac{|I=1\rangle - |I=0\rangle}{\sqrt{2}}$$

so that the elastic and charge-exchange amplitudes are given by

$$\mathscr{T}(\bar{\mathrm{p}}\mathrm{p} \to \bar{\mathrm{p}}\mathrm{p}) = \tfrac{1}{2}(\mathscr{T}^{1}_{\bar{\mathrm{N}}\mathrm{N}} + \mathscr{T}^{0}_{\bar{\mathrm{N}}\mathrm{N}}), \quad \mathscr{T}(\bar{\mathrm{p}}\mathrm{p} \to \bar{\mathrm{n}}\mathrm{n}) = \tfrac{1}{4}(\mathscr{T}^{1}_{\bar{\mathrm{N}}\mathrm{N}} - \mathscr{T}^{0}_{\bar{\mathrm{N}}\mathrm{N}})$$

G-parity

G-parity is a multiplicative quantum number that results from the generalization of C-parity to multiplets of particles. The G-parity operator is defined as

$$\mathcal{G} = \mathcal{C}\, e^{(i\pi I_2)}$$

G-parity is a combination of charge conjugation and a π rad rotation around the 2nd axis of isospin space. Weak and electromagnetic interactions are not invariant under G-parity.

a little bit of history

Nucleon-Antinucleon Optical Potential

J. Côté,[a] M. Lacombe, B. Loiseau, B. Moussallam, and R. Vinh Mau
Division de Physique Théorique, Institut de Physique Nucléaire, F-91406 Orsay, France, and Laboratoire de Physique Théorique et des Particules Elementaires, Université Pierre et Marie Curie, F-75230 Paris Cédex 05, France

PRL 48 (1982) 1320

Antinucleon-nucleon potential

P. H. Timmers, W. A. van der Sanden, and J. J. de Swart
Institute for Theoretical Physics, University of Nijmegen, Nijmegen, The Netherlands

PRD 29 (1984) 1928

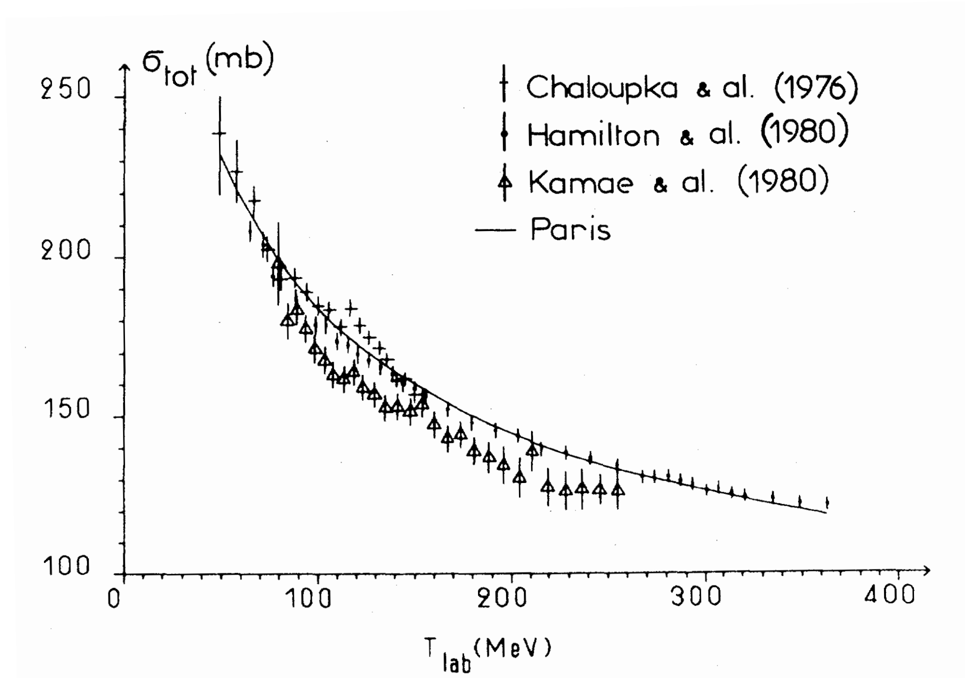

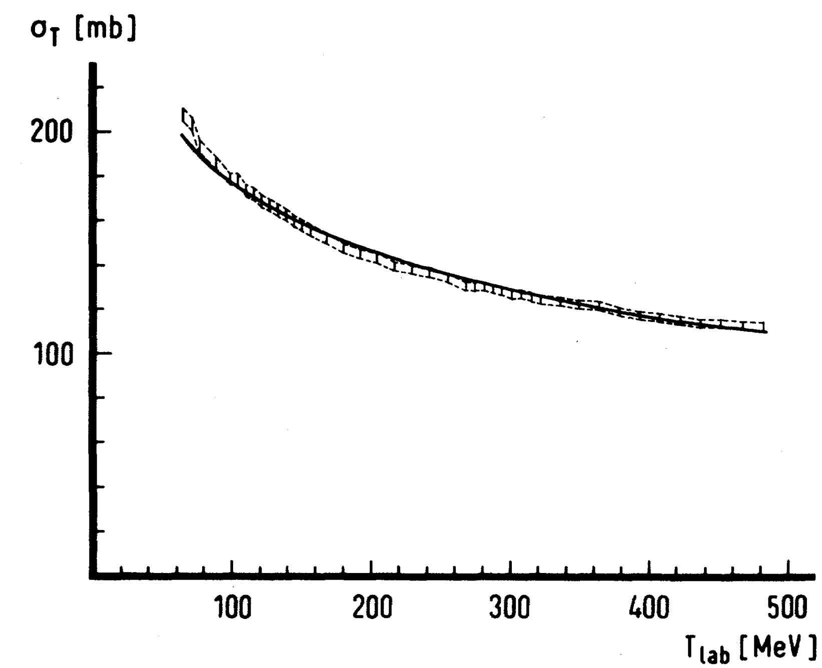

The $\bar{N}N$ potential can be decomposed as follows in three contributions $\mathbf{V = U_S + U_L - i\,W}$:

- $\mathbf{U_S}$, long-range and medium range part generated by G-parity transformation of the Paris potential
- $\mathbf{U_L}$, the short-range component is described phenomenologically (quadratic function)
- **W** an absorptive part that is short-range and energy dependent

$$W_{N\bar{N}}(\vec{r},T_L)=\left(g_C(1+f_C T_L)+g_{SS}(1+f_{SS}T_L)\vec{\sigma}_1\cdot\vec{\sigma}_2+g_T S_{12}+\frac{g_{LS}}{4m^2}\vec{L}\cdot\vec{S}\frac{1}{r}\frac{d}{dr}\right)\frac{K_0(2mr)}{r}$$

The $\bar{N}N$ potential is generated by a G-parity-transformed Nijmegen model-D potential plus a phenomenological short-range potential:

$$V_{ph}(r)=\left[V_C+V_{SS}\vec{\sigma}_1\cdot\vec{\sigma}_2+V_T S_{12}m_e r + V_{SO}\vec{L}\cdot\vec{S}\frac{1}{m_e{}^2 r}\frac{d}{dr}\right]V_{WS}(r)$$

$$V_{WS}(r)=\frac{1}{1+\exp(m_e r)}$$

the most recent Plane Wave Analysis

Energy-dependent partial-wave analysis of all antiproton-proton scattering data below 925 MeV/*c*

Daren Zhou and Rob G. E. Timmermans
KVI, Theory Group, University of Groningen, Zernikelaan 25, NL-9747 AA Groningen, The Netherlands

PHYSICAL REVIEW C **86**, 044003 (2012)

- Energy-dependent partial-wave analysis of all antiproton-proton elastic ($\bar{p}p \rightarrow \bar{p}p$) and charge-exchange ($\bar{p}p \rightarrow \bar{n}n$) scattering data below 925 MeV/c antiproton laboratory momentum.
- The relevant long-range parts of the electromagnetic and the one- and two-pion exchange interactions are included exactly, where the short-range interactions, including the coupling to the mesonic annihilation channels, are parametrized by a complex boundary condition at a radius of r = 1.2 fm.
- They concluded that chiral effective field theory provides an excellent long-range antinucleon-nucleon interaction.

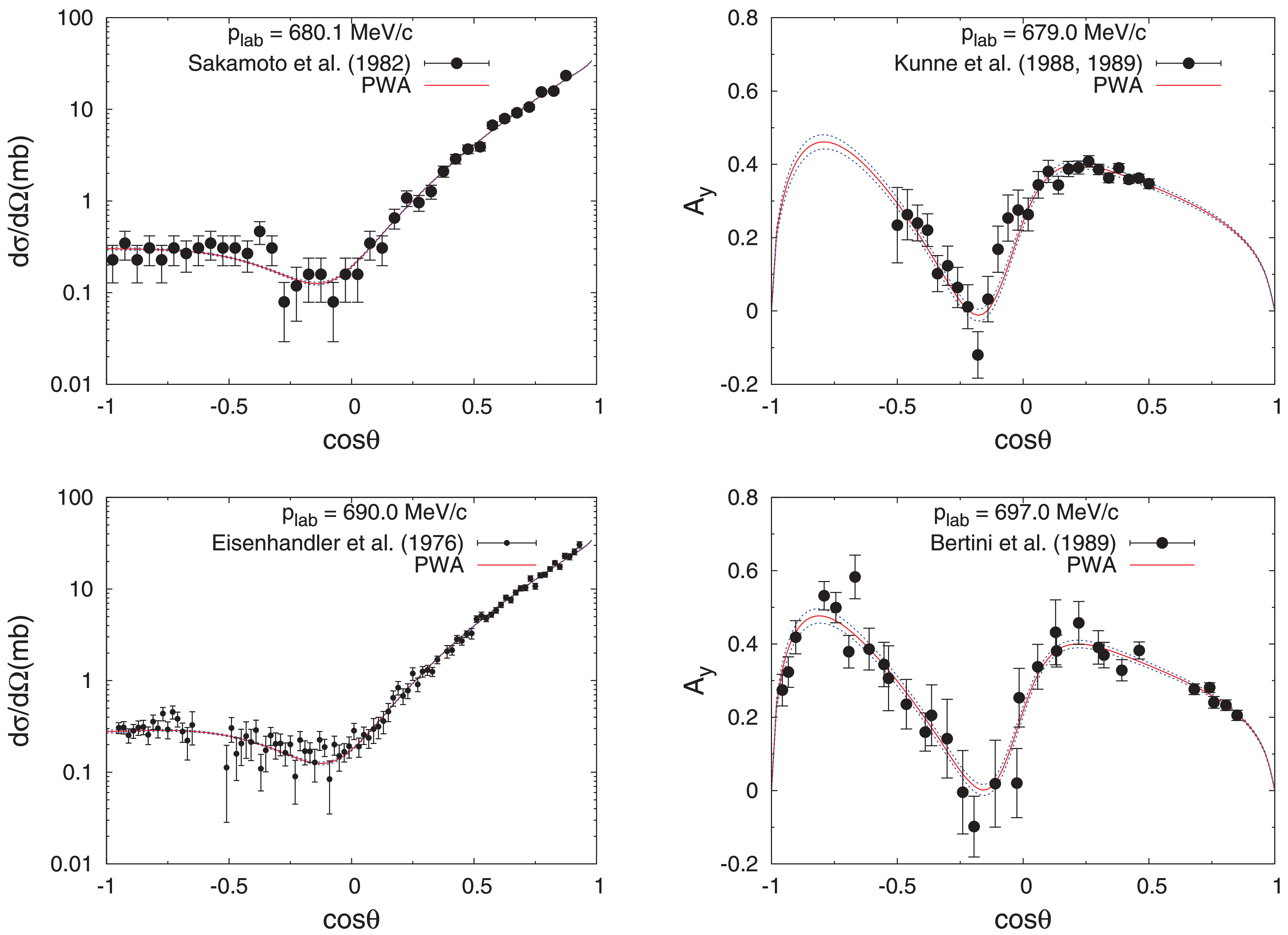

$\bar{N}N$ potentials from ChPT

Antinucleon-nucleon interaction at next-to-next-to-next-to-leading order in chiral effective field theory

JHEP 07 (2017) 078

Ling-Yun Dai,[a] Johann Haidenbauer[a] and Ulf-G. Meißner[a,b]

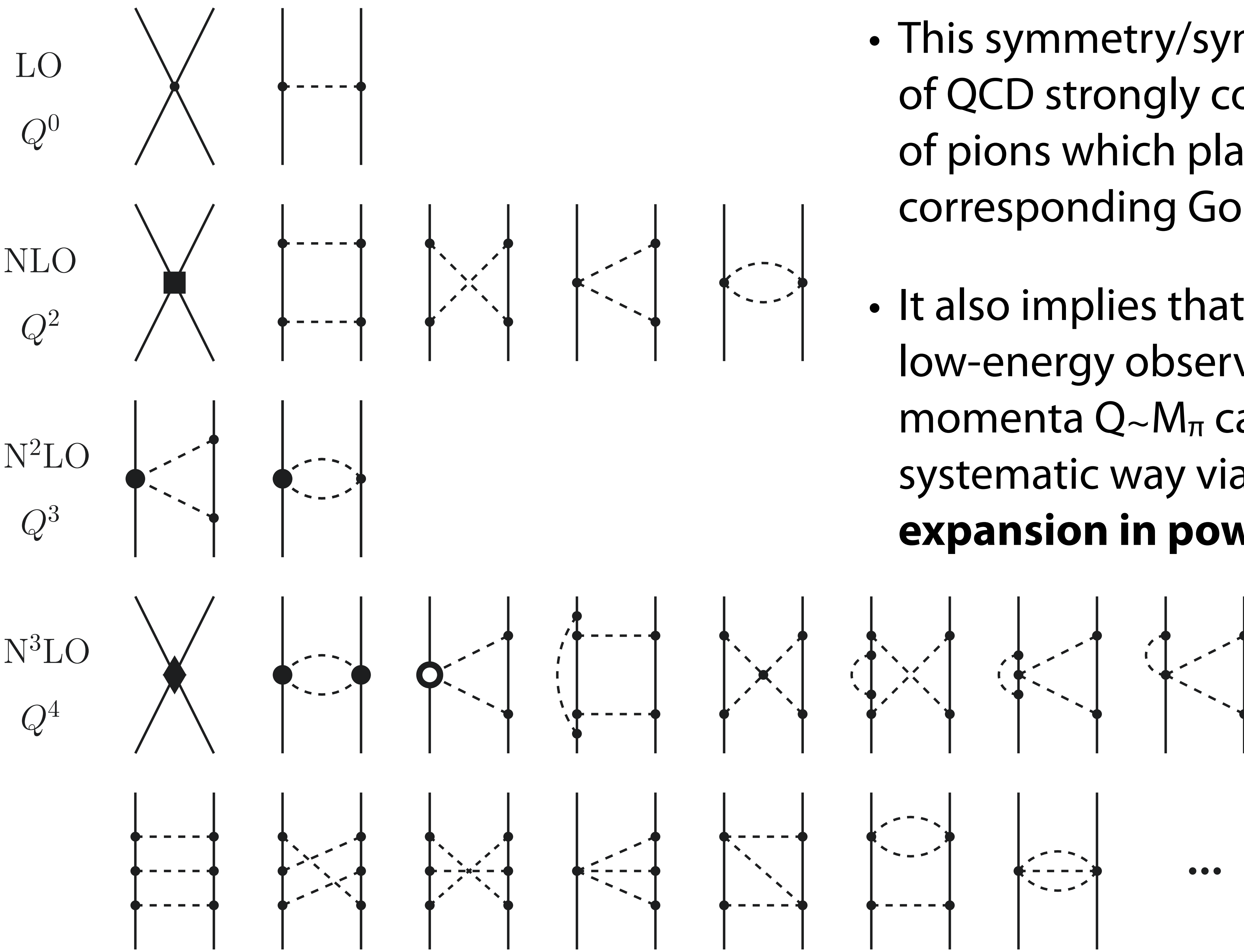

- **Chiral EFT** relies heavily on the approximate spontaneously broken chiral symmetry of QCD.
- This symmetry/symmetry-breaking pattern of QCD strongly constrains the interaction of pions which play the role of the corresponding Goldstone bosons.
- It also implies that pion- and pion-nucleon low-energy observables at external momenta $Q \sim M_\pi$ can be computed in a systematic way via a **perturbative expansion in powers of Q/Λ_χ**

see Haidenbauer's talk tomorrow

$\bar{N}N$ potentials from ChPT

Antinucleon-nucleon interaction at next-to-next-to-next-to-leading order in chiral effective field theory

JHEP 07 (2017) 078

Ling-Yun Dai,[a] Johann Haidenbauer[a] and Ulf-G. Meißner[a,b]

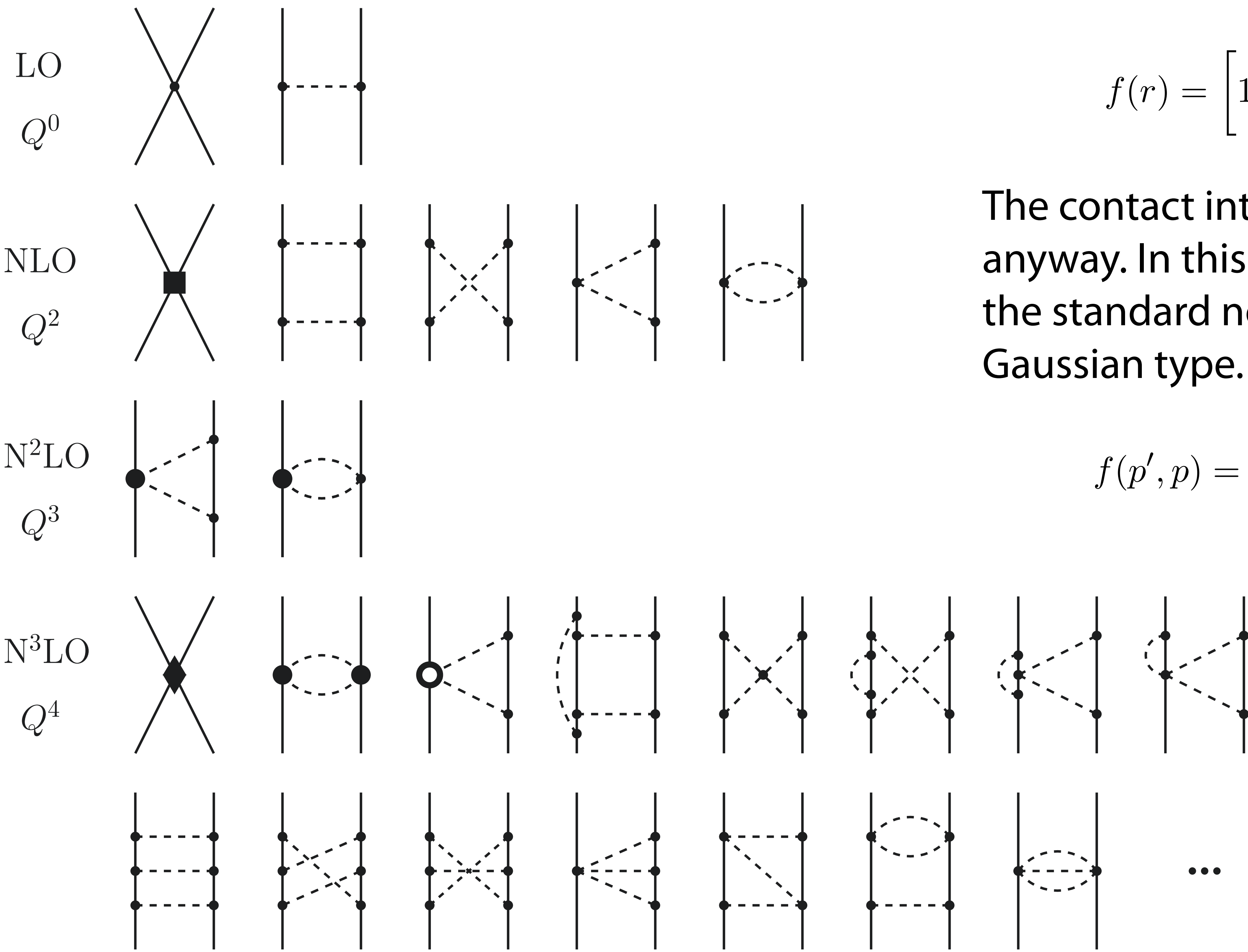

A new local regularization scheme has been used for the pion-exchange contributions

$$f(r) = \left[1 - \exp\left(-\frac{r^2}{R^2}\right)\right]^n$$

The contact interactions are non-local anyway. In this case they use again the standard nonlocal regulator of Gaussian type.

$$f(p', p) = \exp\left(-\frac{p'^m + p^m}{\Lambda^m}\right)$$

see Haidenbauer's talk tomorrow

$\bar{N}N$ potentials from ChPT

JHEP 07 (2017) 078

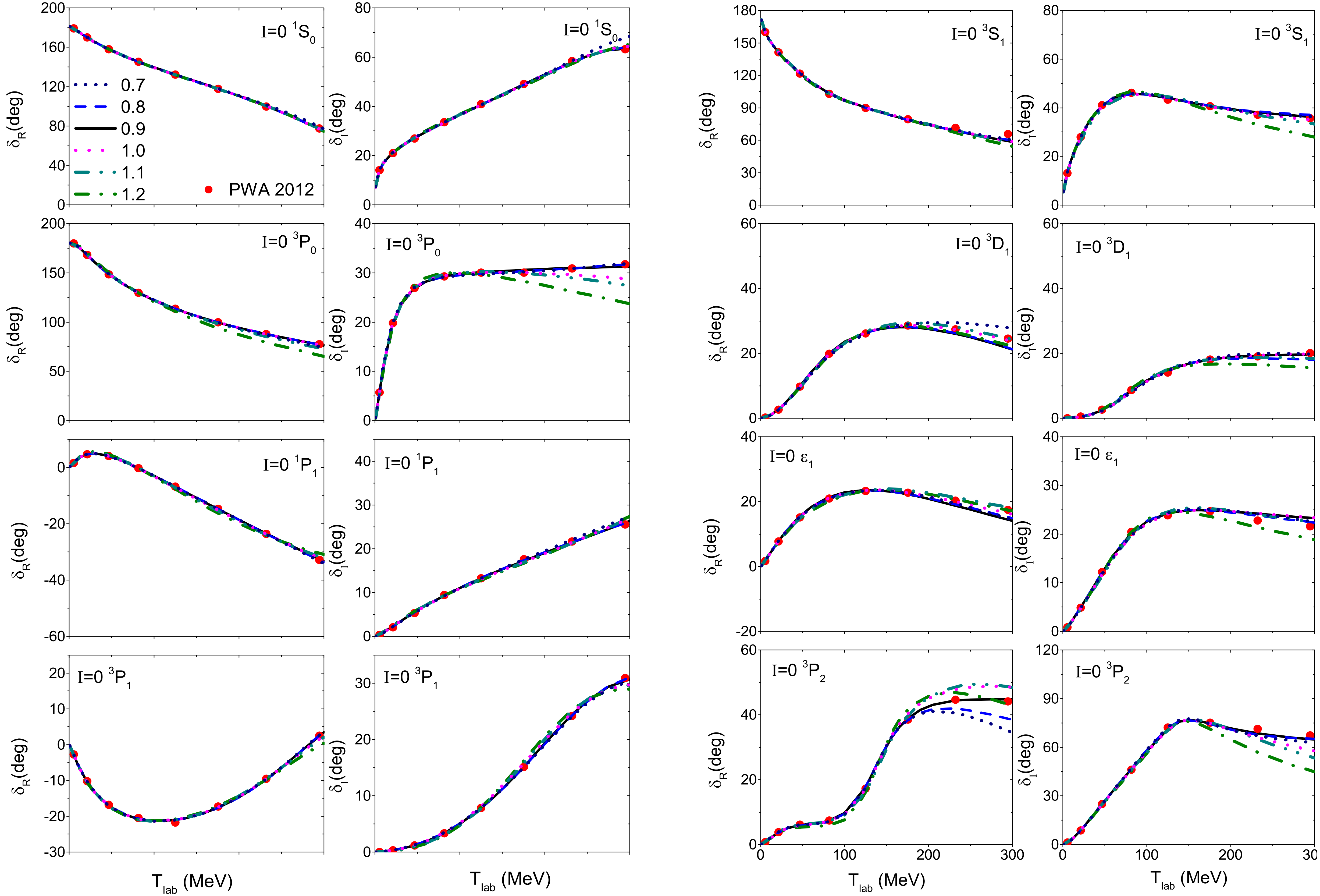

Real and imaginary parts of various $\bar{N}N$ phase shifts at N^{3}LO for cutoffs R = 0.7 – 1.2 fm

Benchmarks

nucleon-nucleus elastic scattering

elastic proton scattering off Oxygen 16

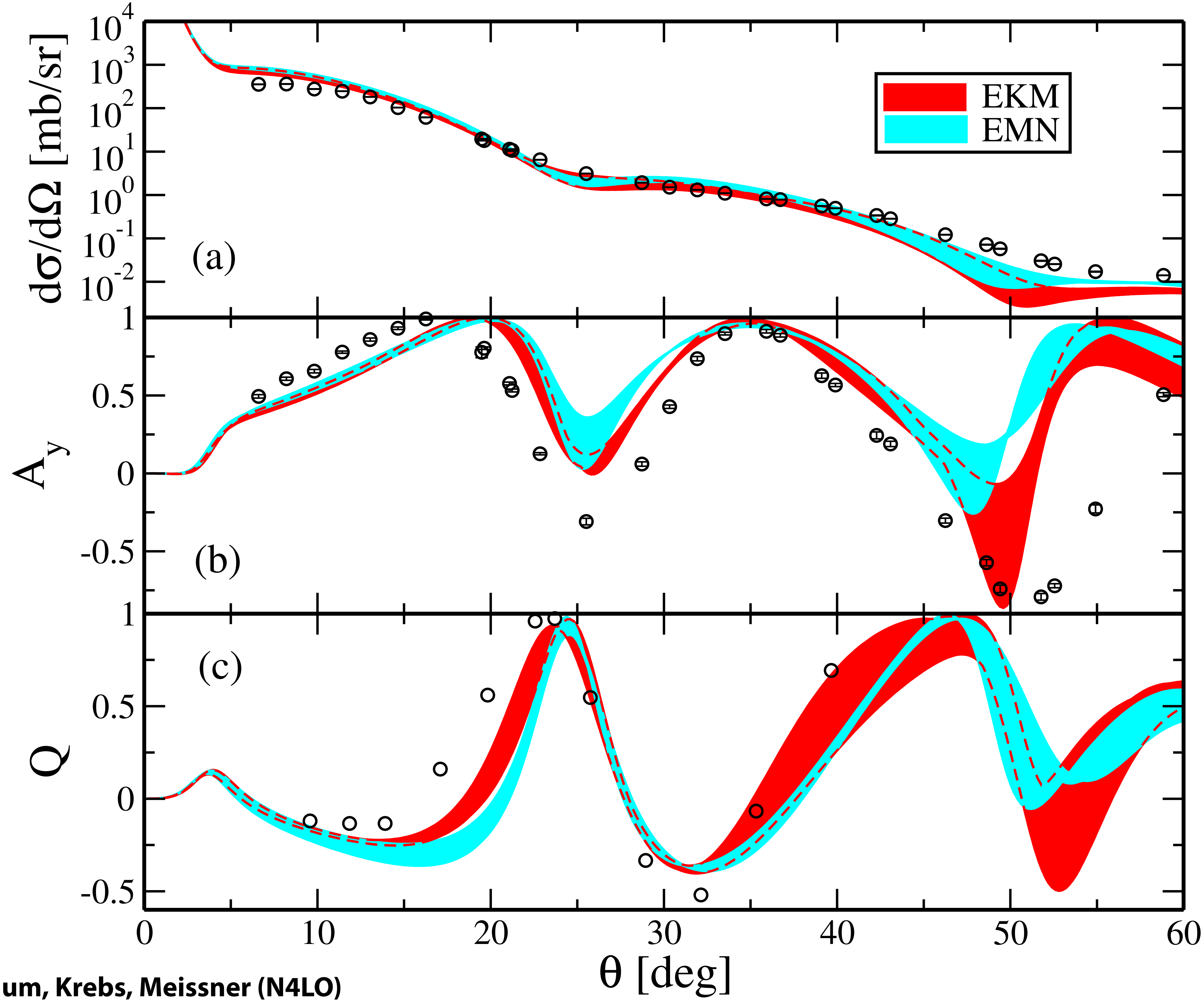

EKM = Epelbaum, Krebs, Meissner (N4LO)
EMN = Entem, Machleidt, Nosyk (N4LO)

Phys. Rev. C 96 (2017) 044001

what about convergence?

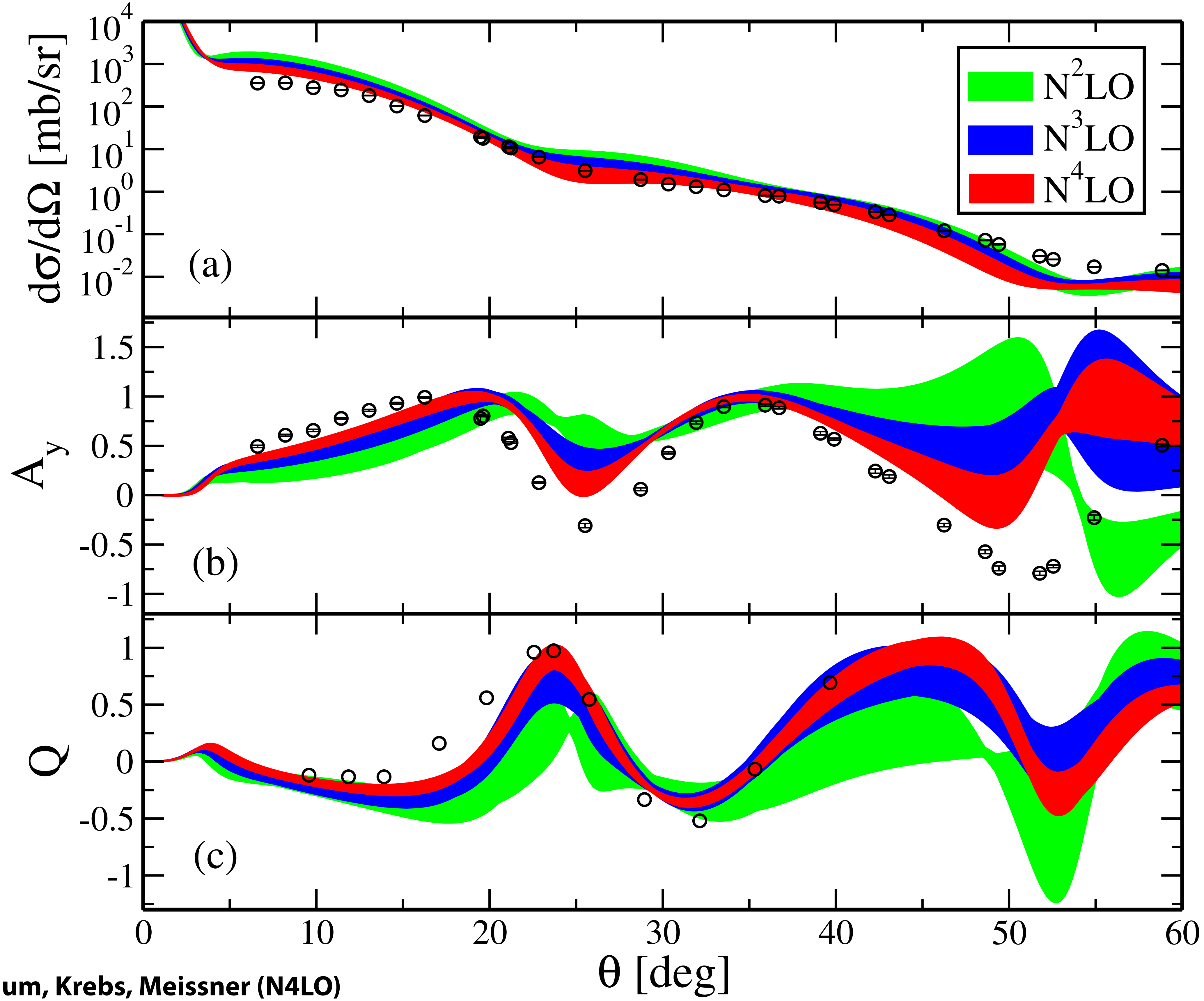

EKM = Epelbaum, Krebs, Meissner (N4LO)

EMN = Entem, Machleidt, Nosyk (N4LO)

Phys. Rev. C 96 (2017) 044001

microscopic vs. phenomenological

KD: A. J. Koning and J. P. Delaroche, Nucl. Phys. A713, 231 (2003)

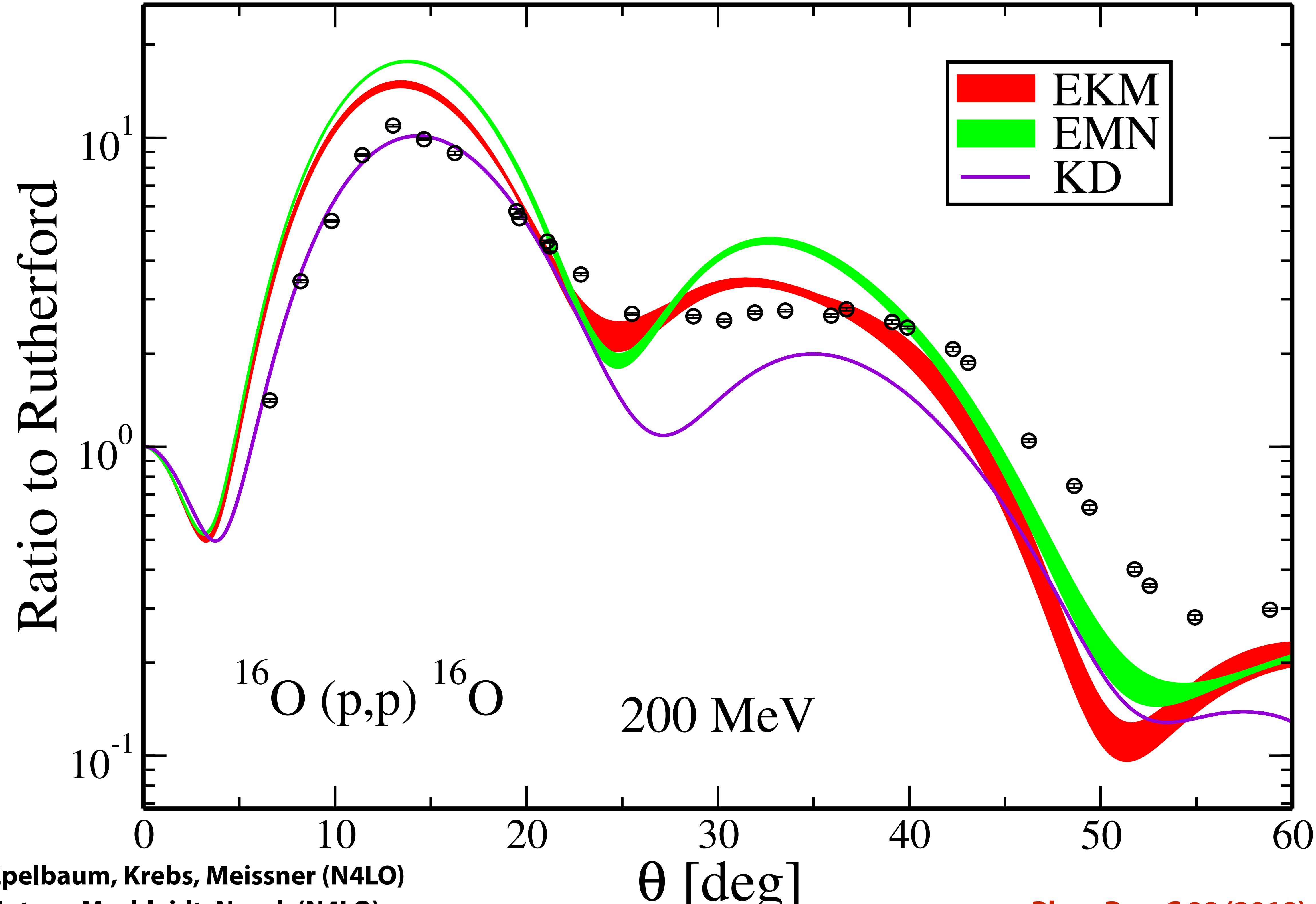

EKM = Epelbaum, Krebs, Meissner (N4LO)
EMN = Entem, Machleidt, Nosyk (N4LO)

Phys. Rev. C 98 (2018) 064602

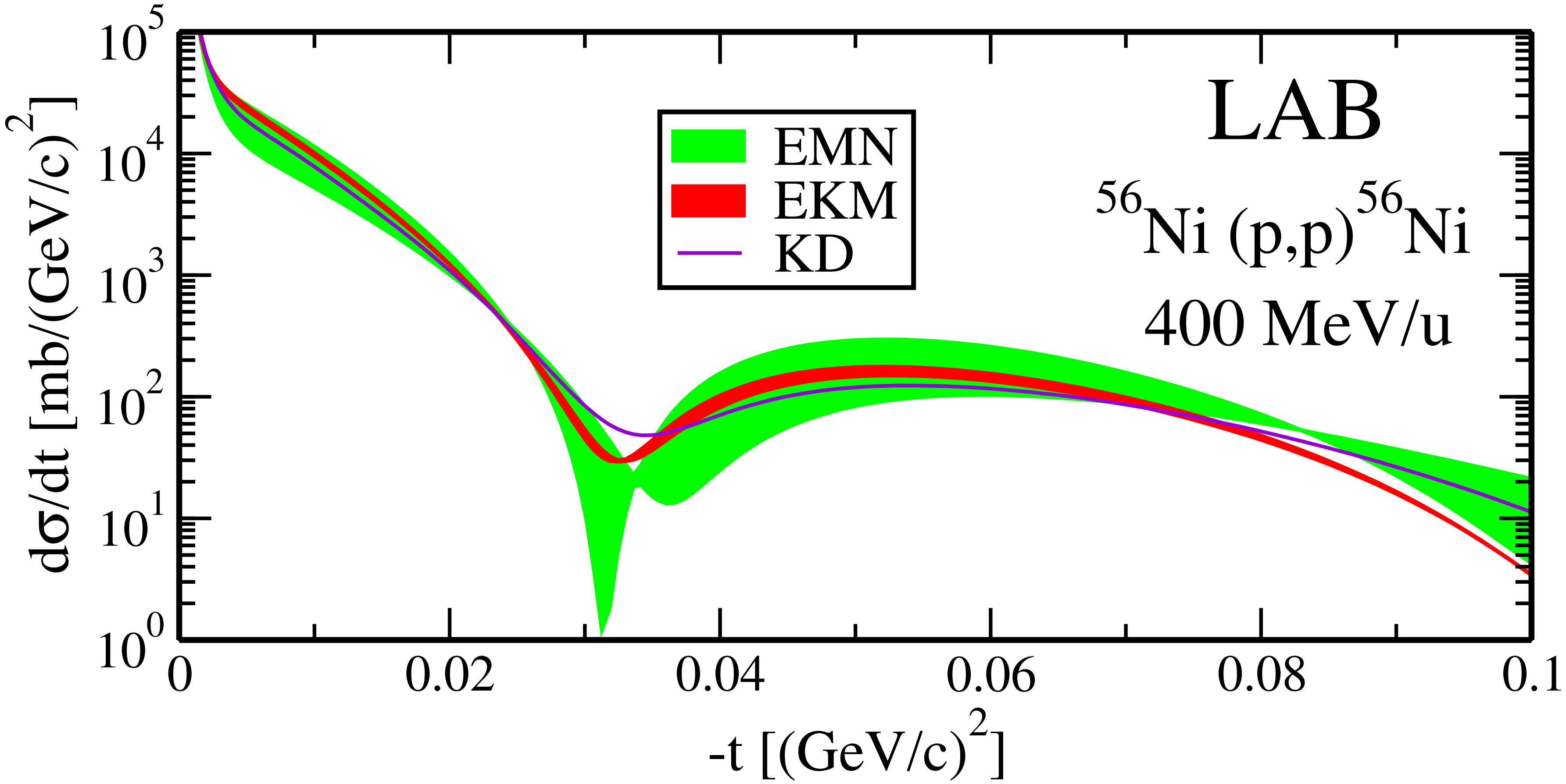

Phys. Rev. C 98 (2018) 064602

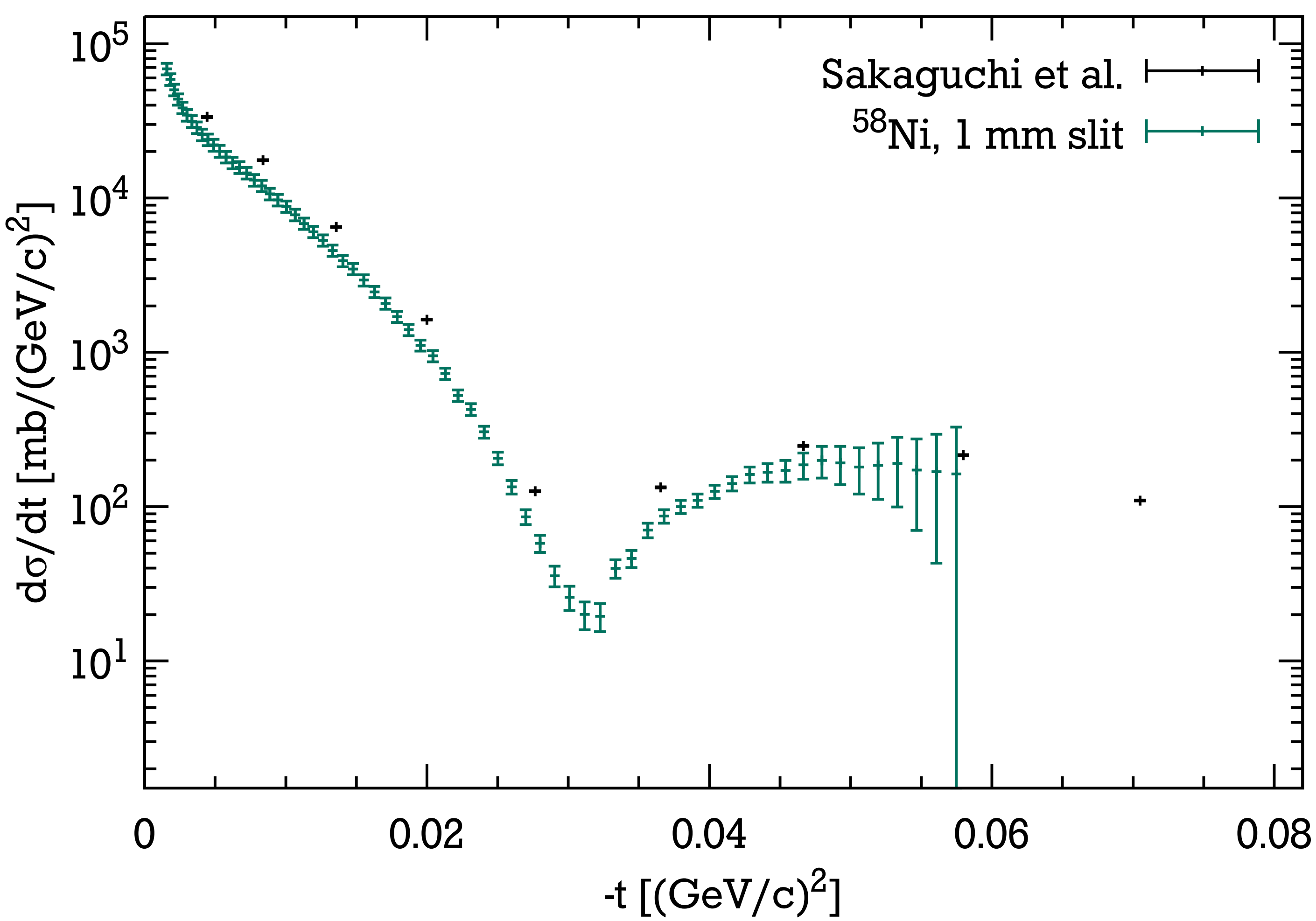

Nuclear matter distribution of ^{56}Ni measured with EXL

Kerndichteverteilung von ^{56}Ni gemessen mit EXL
Vom Fachbereich Physik der Technischen Universität Darmstadt zur Erlangung des Grades eines Doktors der Naturwissenschaften (Dr. rer. nat.)
genehmigte Dissertation von Mirko von Schmid M.Sc. aus Fulda
2015 — Darmstadt — D 17

TECHNISCHE UNIVERSITÄT DARMSTADT

Fachbereich Physik
Institut für Kernphysik
AG Kröll

Results

elastic antiproton scattering off light nuclei

what about convergence?

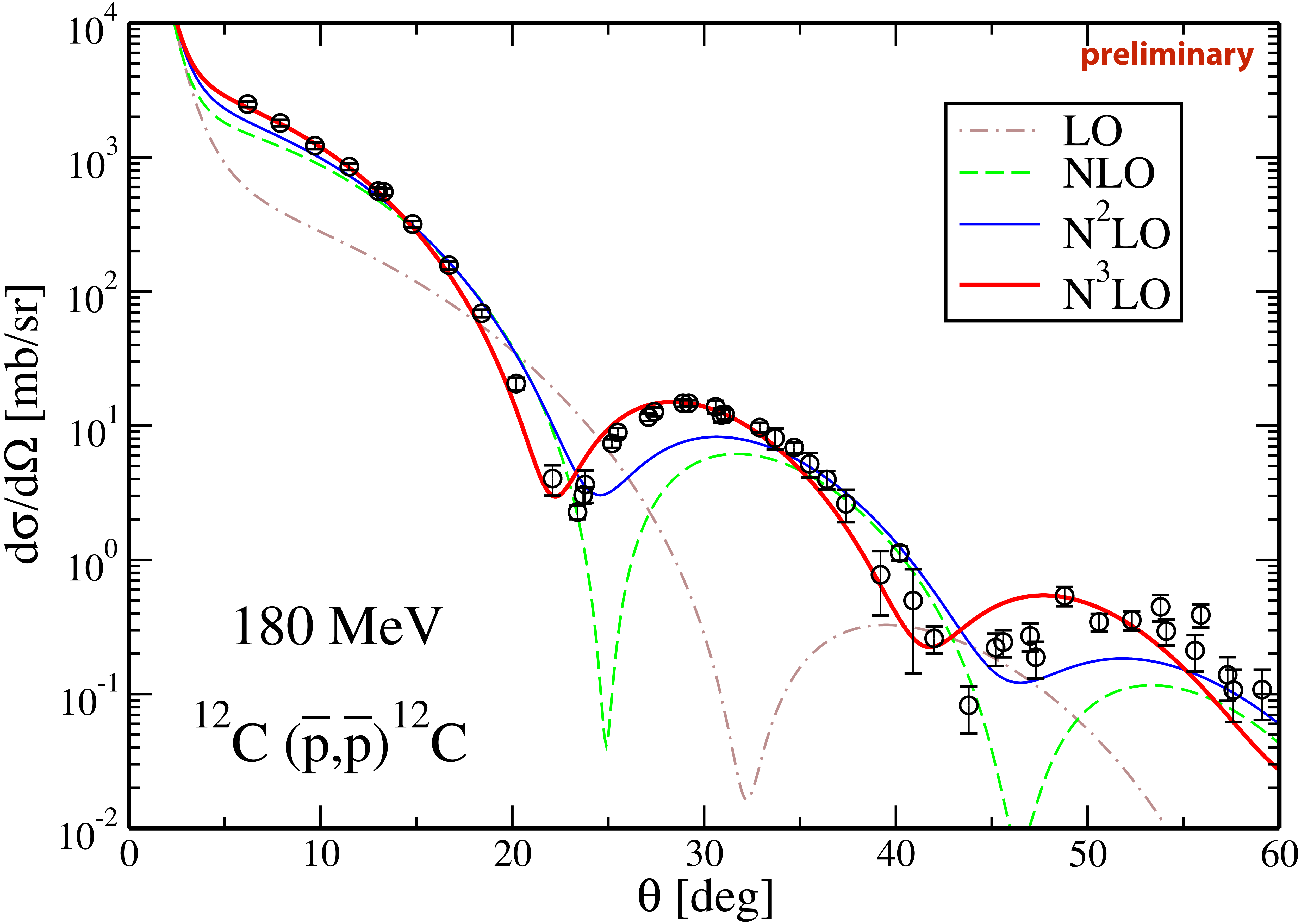

Helium 4

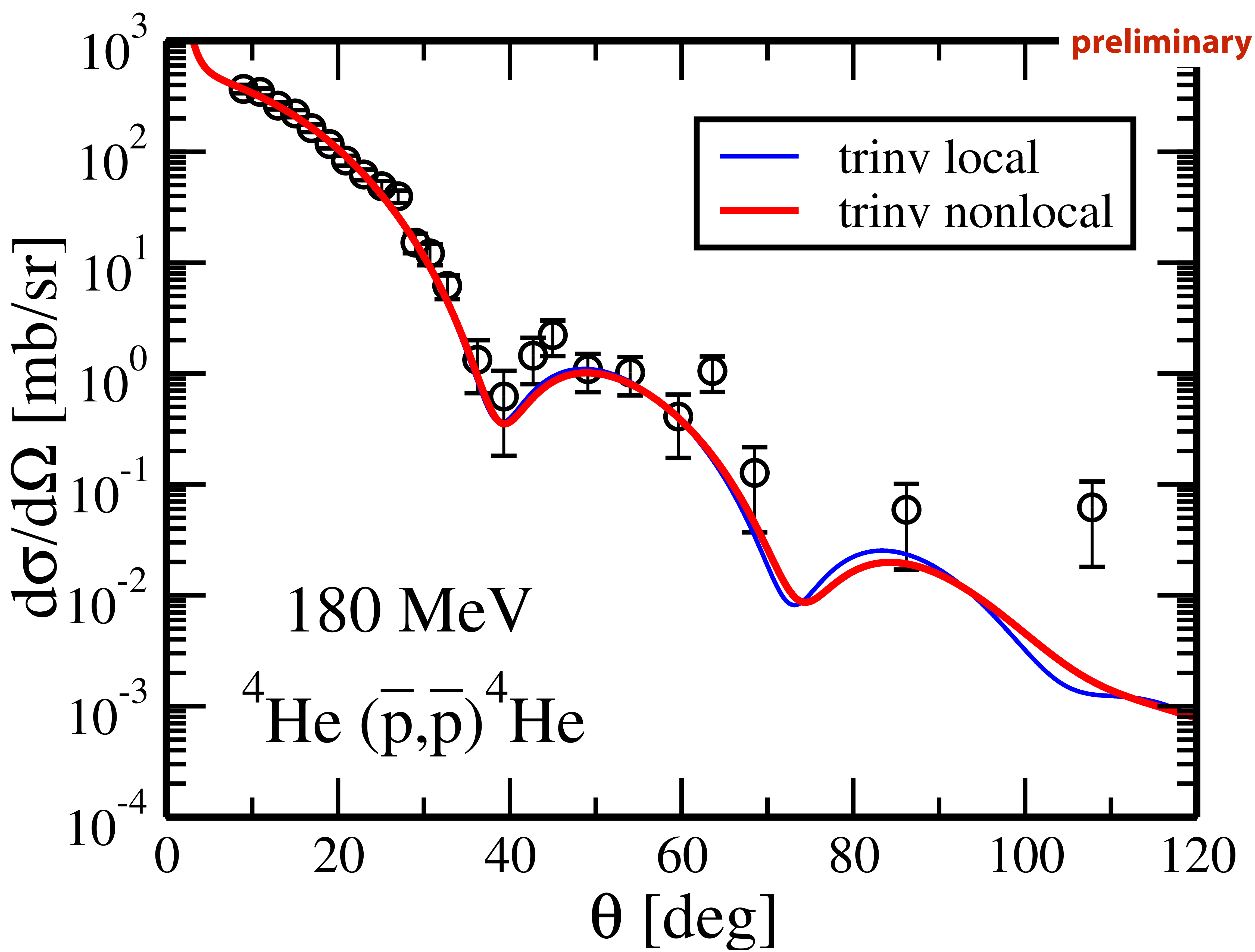
preliminary
trinv local
trinv nonlocal
180 MeV
^{4}He ($\bar{p}$,$\bar{p}$) ^{4}He
dσ/dΩ [mb/sr]
θ [deg]
10^3
10^2
10^1
10^0
10^{-1}
10^{-2}
10^{-3}
10^{-4}
0
20
40
60
80
100
120

Carbon 12

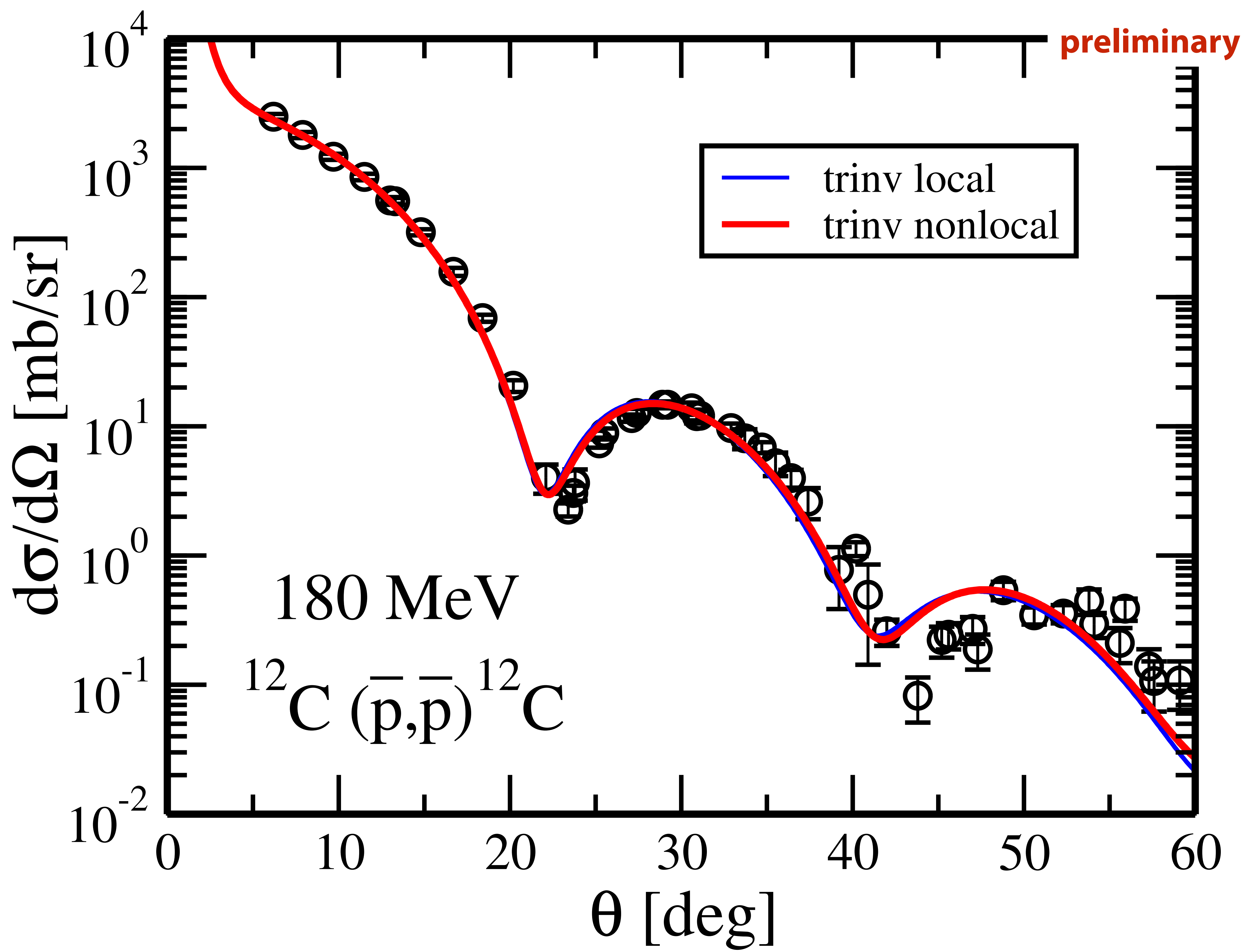
preliminary
trinv local
trinv nonlocal
180 MeV
$^{12}C(\bar{p},\bar{p})^{12}C$
$d\sigma/d\Omega$ [mb/sr]
θ [deg]
10^4
10^3
10^2
10^1
10^0
10^{-1}
10^{-2}
0
10
20
30
40
50
60

Oxygen 16

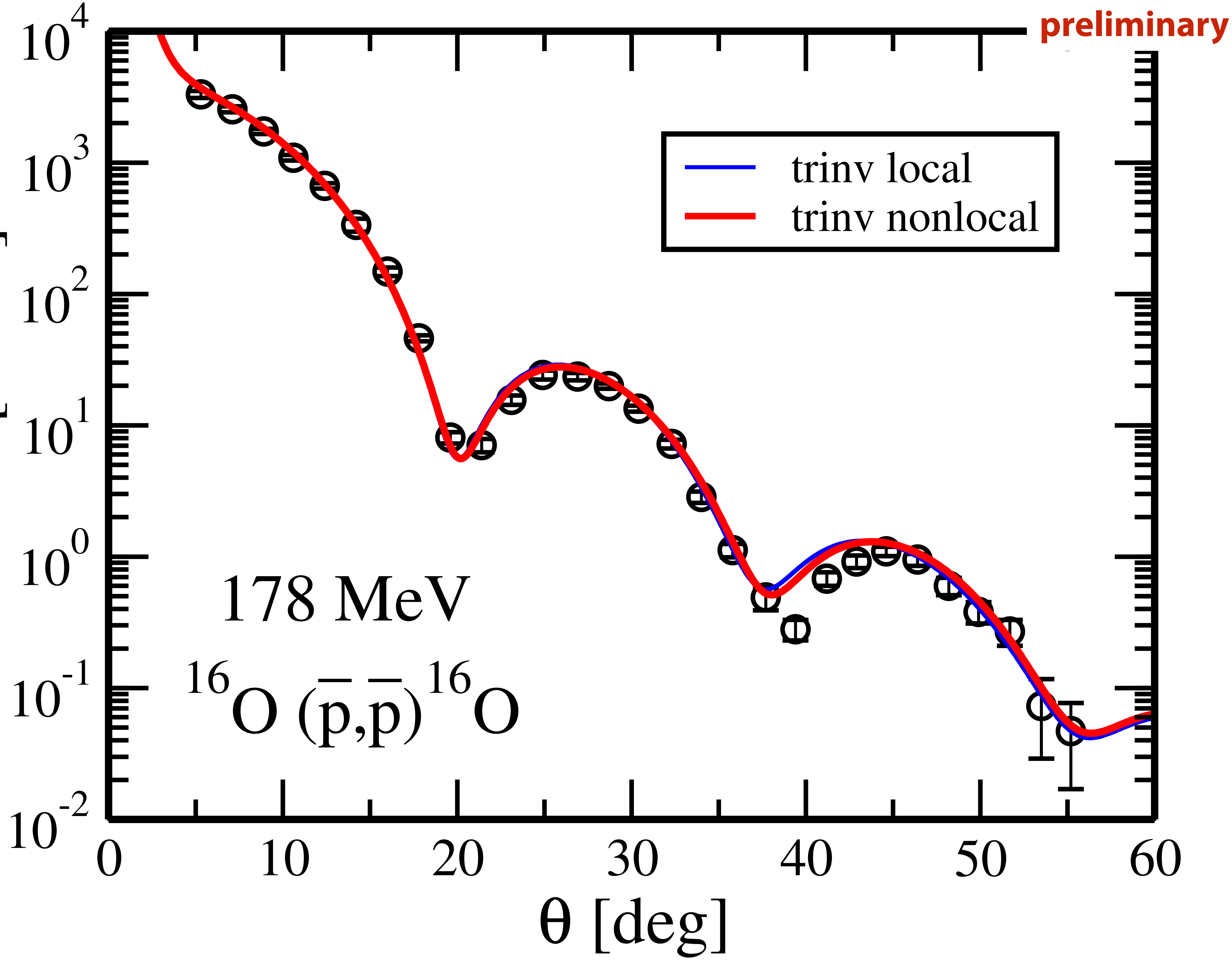
preliminary
trinv local
trinv nonlocal
178 MeV
$^{16}O\,(\bar{p},\bar{p})\,^{16}O$
$d\sigma/d\Omega$ [mb/sr]
θ [deg]
10^{4}
10^{3}
10^{2}
10^{1}
10^{0}
10^{-1}
10^{-2}
0
10
20
30
40
50
60

Oxygen 18

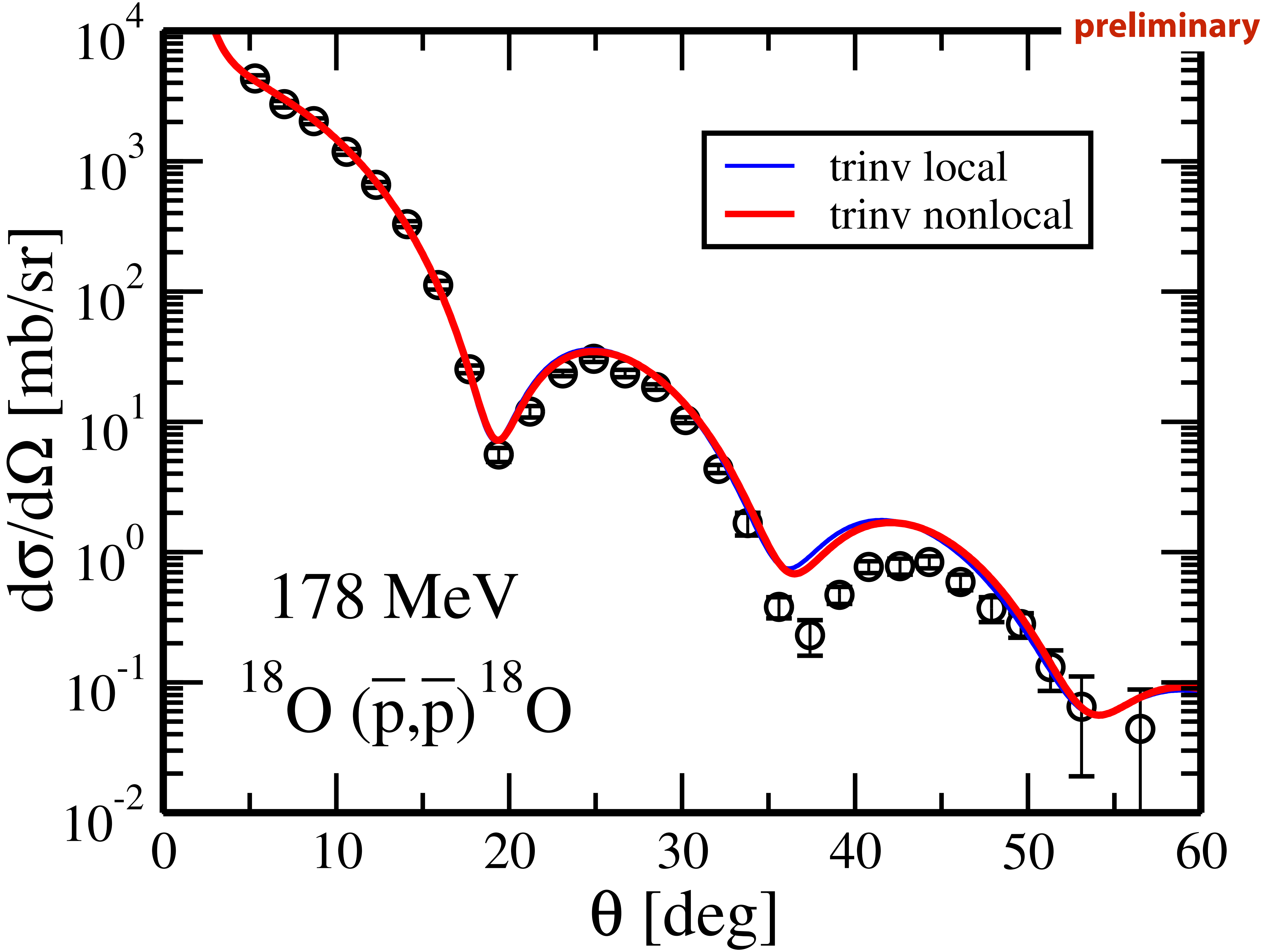

preliminary
trinv local
trinv nonlocal
178 MeV
$^{18}O(\bar{p},\bar{p})^{18}O$
dσ/dΩ [mb/sr]
θ [deg]
10^{4}
10^{3}
10^{2}
10^{1}
10^{0}
10^{-1}
10^{-2}
0
10
20
30
40
50
60

Light nuclei with DFT densities

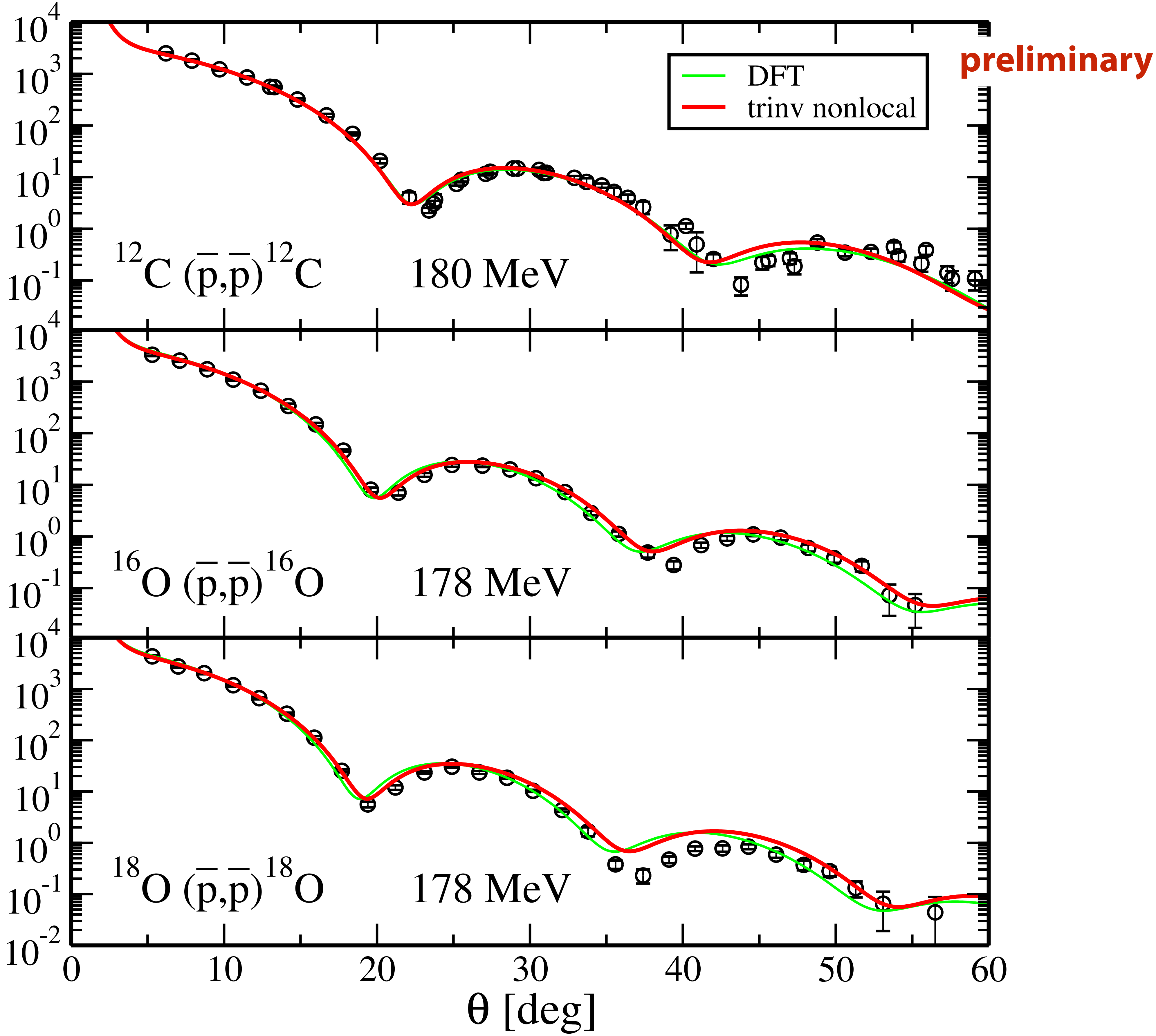

Heavier nuclei (only DFT)

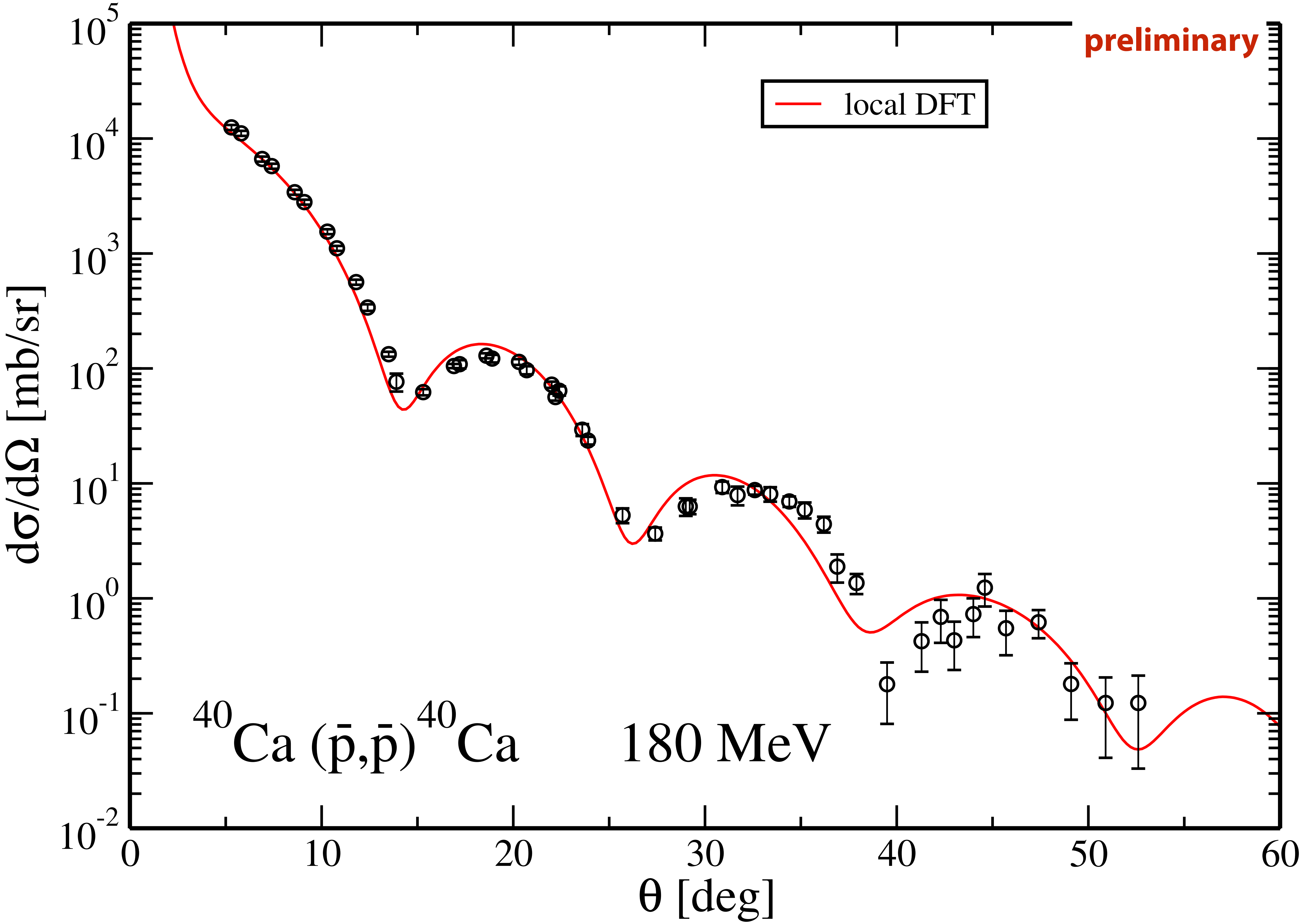

Heavier nuclei (only DFT)

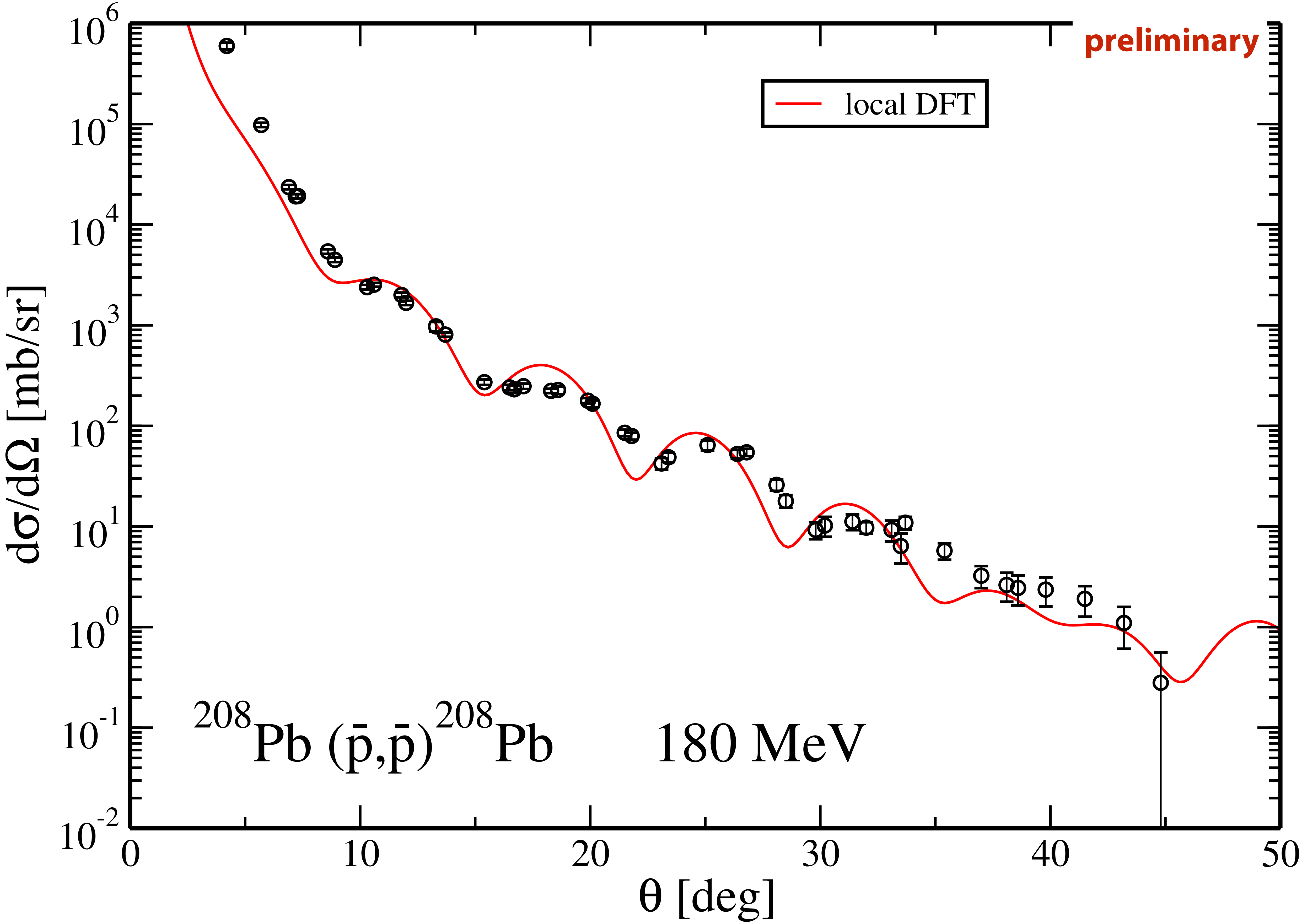

Conclusions

- For the first time, a **full microscopic** description of elastic antiproton scattering off light nuclei
- In-medium contributions and many-body forces appear to be rather small

Remarks

- Spin observables still to be fully calculated but they look like under control
- To describe low-energy observables, the impulse approximation has to improved
- Annihilation processes in the near future